

APPENDIX D

SUMMARY OF NOVEMBER 1986 NSF REVIEW

The following is a copy of the title page and Summary from "Report to the National Science Foundation by the Panel on Interferometric Observatories for Gravitational Waves," which was submitted to NSF in January 1987 after a one-week (November 1986) review of the LIGO Project.

Report to the National Science Foundation

by the

Panel on Interferometric Observatories for Gravitational Waves

January 1987

5. SUMMARY

- A) A strong case has been made for the scientific value of the goals of the project.
- B) Though there are large uncertainties associated with the strengths of the many different kinds of astrophysical sources and the ultimate capability of interferometric detectors, there is a high probability that this facility will ultimately provide for a giant leap in our understanding of the gravitational force, one of the most fundamental forces of nature, as well as our knowledge of astrophysical phenomena.
- C) It is anticipated that this facility would uniquely provide the most sensitive and certain prospect for detecting astrophysical events and identifying their nature. Essential to this capability is the twin nature of the two interferometers. Though companion efforts in other countries are highly desirable, a common management of the two LIGO detectors is important both for the coordination of the observational program and for the analysis and identification of observed events. This facility would provide for a continued and thriving development of the field.
- D) It is important to proceed directly to the construction of a long baseline interferometer in a timely manner since many aspects of the detector development program cannot otherwise be tested.
- E) The rate of detectable extragalactic events increases as the cube of the interferometer sensitivity, thus putting a high premium on the long baseline. Though a multistage, or phased authorization to the final configuration was carefully considered, the panel does not recommend this approach. We recommend full authorization with phased construction and appropriate milestones.
- F) The plans as described in the presentations and in the various documents provided appear to be well conceived. The procedure which has been employed in drawing up the existing designs and in making the cost estimates appears reasonable and adequate for proceeding to the final design for submission. Effort should continue to examine design alternatives which may decrease costs, particularly in the area of the vacuum system and enclosure. We do not recommend that the project be delayed by this process of re-examination. It is important to make the choice between Fabry-Perot and Michelson interferometer type detectors before submission of the final design. However, it remains important to develop advanced detectors and therefore research should continue to this end.
- G) Because of the magnitude and dual nature of the facility, with laboratory sites widely separated, it is especially important that the construction and operation be well managed. The panel feels that the project requires a single scientific project leader of high stature to direct the activities. Efforts should immediately be directed to providing such leadership.
- H) In looking forward to the utilization of the facilities it should be recognized that in addition to a budget for its operation, adequate funds will be required to support both the needs of experimental groups and further detector development.

I) In conclusion, the panel enthusiastically supports this development effort and urges that the plans for the project be refined along the lines indicated and that the design be completed. We recommend, then, that the construction project be brought to the National Science Foundation Board for consideration and (hopefully) for funding.

Panel Members:

Daniel B. DeBra
Val L. Fitch
Richard L. Garwin
John L. Hall

Boyce D. McDaniel
Andrew M. Sessler
Saul A. Teukolsky
Alvin A. Tollestrup

APPENDIX E

OTHER PROGRAMS IN GRAVITY WAVE OBSERVATIONS

Several other types of gravitational wave detectors are under development [E-1]. The timing of pulsars (comparison of rotation rates of distant neutron stars with ticking rates of atomic clocks on earth) has produced cosmologically interesting limits on extremely low frequency gravitational waves ($f \sim 10^{-7}$ to 10^{-8} Hz) [E-2]. NASA's doppler tracking of spacecraft is being used to search for low-frequency waves ($f \sim 10^{-1}$ to 10^{-4} Hz) [E-3]; and feasibility studies are being carried out [E-4] for interferometric detectors, like those in the LIGO, which would fly in space and replace doppler tracking in the low-frequency band. In the high-frequency band, $f \sim 10$ Hz to 10^4 Hz, in addition to the interferometric detectors that we are developing, there are earth-based bar detectors in which the gravitational wave drives a normal mode of vibration of a solid bar of aluminum, niobium or sapphire, and an electromechanical transducer monitors that mode [E-5]. Bar detectors are discussed in Part II.D.

Interferometric detectors are under development elsewhere in the world [E-1]. In 1977 the Max Planck Institute in Munich, West Germany initiated an interferometric effort under the leadership of H. Billing, and Glasgow University initiated an effort under the leadership of R. W. P. Drever. Since Drever joined Caltech, the Glasgow effort has been led by James Hough. The Max Planck group initially developed a 3-meter delay-line prototype receiver, then after several years expanded to a 30-meter system at Garching. Glasgow University began with a short delay-line testbed, then switched to a 10-meter Fabry-Perot. The present performance of the different interferometric systems is comparable. In terms of strain sensitivity (i.e. \tilde{h}), the 40-meter system has the best performance at frequencies above 500 Hz, while the Max Planck system is better at lower frequencies. In terms of displacement sensitivity, the Glasgow system is about three times better than any of the other systems at frequencies above 1 kHz.

In 1983 Alain Brillet initiated an interferometric effort in Orsay France. Since then he and his group have focussed primarily on the development of high-intensity, highly frequency-stable laser sources, an effort of considerable importance for us and the other groups. In 1985 Nabuki Kawashima initiated an interferometric effort at the Institute of Space and Aeronautical Science in Tokyo; and in 1987 a group under Adalberto Giazotto in Pisa Italy, working on antiseismic isolation, initiated a collaborative agreement with the French group for interferometric work.

There are strong interactions between the American, European, and Japanese interferometric groups, including occasional exchanges of personnel; and we expect those interactions to increase as time passes. (See the discussion of National and International Cooperation in Appendix C.) We are hopeful, but not certain, that the Europeans will construct one or two full-scale interferometric systems sufficiently rapidly to provide, with the American LIGO, a sizable fraction of the world-wide network which is required for extraction of full information from the waves. On a longer timescale, we hope for a Japanese or Australian completion of the network. (Cf. the discussion of sites in Appendix B.)

REFERENCES

- E-1. For a general review, see e.g., Kip S. Thorne, "Gravitational Radiation", in *300 Years of Gravitation*, edited by S. W. Hawking and Werner Israel (Cambridge University Press, Cambridge, England), pp. 330–458; available in preprint form from Kip S. Thorne, 130-33 Caltech, Pasadena, CA 91125.
- E-2. Joseph H. Taylor, in *Proceedings of the Eleventh International Conference on General Relativity and Gravitation*. (Cambridge University Press, Cambridge, 1987).
- E-3. Frank B. Estabrook, *Acta Astronautica*, in press.
- E-4. J. E. Faller, P. L. Bender, J. L. Hall, D. Hils, and M. A. Vincent, in *Proceedings of the Colloquium "Kilometric Optical Arrays in Space"*, Cargese (Corsica), 23–25 October 1984. ESA SP-226.
- E-5. P. F. Michelson, J. C. Price, and R. C. Taber, *Science*, **237**, pp. 150–157, 10 July 1987.

APPENDIX F

PRELIMINARY DESIGN OF A LIGO FABRY-PEROT RECEIVER

F.1 Introduction

In Section V-A.1 of this proposal an outline is given of some of the basic ideas of a Fabry-Perot gravity-wave detector and of the status of the current experimental work. The experimental development of succeeding variants of this instrument over the 8 years since the idea was conceived has given a strong background of practical experience, and it is now a sophisticated piece of apparatus. We have now reached a stage where it is possible to design in considerable detail a Fabry-Perot detector based on our present knowledge which could be operated in the LIGO facilities with a good probability of satisfactory operation, and likely to reach at least the initial sensitivity estimates indicated in Figures A-4a,b,c. An outline of such a design is summarized here, both to give some indication of the kind of instrument we are developing, and also to give a better idea of the technology involved. It should be emphasized that this particular design was intended as an initial receiver to be built at minimum risk with our existing technology, and not the design we would be capable of producing some years from now—when we would have to freeze the design—nor as a design for the highest performance we could currently aim at. It is an essentially simpler design than some in our longer-term plans.

F.2 Goals of the Design

(A) A reasonable compromise between maximum designed sensitivity and avoidance of risk of failure due to excessive dependence on untested technologies.

(B) Design of a relatively simple "Base Model" intended to easily achieve a satisfactory and potentially useful performance for initial operation, but designed also for future enhancements by addition of further components, increasing laser power, etc., to form a variety of compatible future "Upgrades" from which a planned succession of receivers can be chosen. In addition, the possibility of some "Downgrades" from the Base Model is also taken into account, in case development becomes delayed, unexpected problems arise, or cost restrictions force cutbacks in initial performance.

(C) A receiver design which is as compatible as possible with other receivers which may share the vacuum system and operate concurrently. The objective of using or obscuring a minimum area of the cross section of the vacuum pipe has thus been an important factor in the design, so that the maximum number of other receivers, which may have test masses located either behind or in front of its own test masses, may be operated with it. Design choices giving minimum cross sectional area have been adopted wherever possible.

(D) A basic receiver design capable of being realized and enhanced in a way which is economical both in construction cost and in design effort. To this end the construction of the receiver is made modular as far as possible, with most elements common throughout the different versions and upgrades or downgrades. This should allow economies in design effort, and facilitate small-scale quantity production of the main units so that cost

and effort required eventually to put into operation several receivers covering different gravitational wave experiments will be minimized. Also common components are used as far as possible for various functions within any one interferometer, so that items such as test mass blanks and many suspension components can be ordered in quantity.

(E) A receiver system capable of operation over extended periods without manual adjustment. A totally automatic alignment control system is an important feature of the design, as it is felt that this will become an essential operating requirement with any type of interferometer having kilometer-long lever arms in the optical beams. A manual alignment system is however also provided for early test purposes, and as a backup which comes automatically into operation in case of disruption by excessive seismic noise, loss of servo lock, equipment malfunction, or other types of failure.

(F) A general aim is to maximize the probability that the receiver when built will actually operate as planned, and in particular to design an interferometer which will be as immune as practicable to unpredicted phenomena which might reduce sensitivity. To this end the interferometer is designed to hold as constant as possible parameters which otherwise might conceivably introduce noise at frequencies near the gravity wave frequency region. Parameters which are controlled and maintained constant at relevant frequencies in this design include laser beam frequency, intensity, diameter, divergence and spectral composition; beam direction and position parameters in each arm relative to the positions of the test masses; and test mass translational and rotational coordinates. (Differential forces required to maintain the relative distances between the pairs of test masses in each arm constant are recorded as a measure of the gravitational wave.) Precautions taken in the design to control some of the parameters do go further than experience so far with prototype interferometers has shown to be absolutely essential, and it is quite likely that it may later be found to be unnecessary to control all of them as well as is provided for. However building in this control gives additional insurance against quite large classes of unpredicted phenomena.

F.3 Summary of Characteristics of the Base Model Receiver, and Planned Upgrades and Downgrades

Consideration of the goals listed above has led to a design in which initial operation of the basic interferometer is planned with light from a single argon laser, though possibly with additional argon lasers available as backup. This approach requires minimal extension over present prototype operation. Recycling (Section V-A.2b) is proposed as a means of achieving good sensitivity with this relatively low power input, as it is judged that operation in a recycling mode will be easier and have less risk of failure than adding lasers together or use of Nd:YAG lasers. (If Nd:YAG lasers were used it may be advantageous to employ frequency doubling to keep within the wavelength region that allows use of the relatively small low-loss cavity mirrors and test masses proposed here.)

Two versions of the Base Model are contemplated: Version 1, currently proposed as the first interferometer, intended for broadband searches; and Version 2, envisaged as likely to be later unless there is some unexpected development in source estimates or detector technology, optimized for narrowband operation. The proposed main characteristics of these and of their upgrades and downgrades follow.

(A) Base Model, Version 1 (Broadband)

- (1) Light source—one single-mode argon ion laser, giving 5 to 6 watts output at 514 nm. (e.g. Coherent Innova or Spectra-Physics large-frame lasers of nominal all-line power 20 watts).
- (2) Test Masses: Fused Silica, 8 inches diameter by 5 inches long, with ultra-low-loss mirror coating over the front surface giving a minimum usable area 5.5 inches in diameter.
- (3) Test mass suspension giving primarily passive seismic isolation, but with a slaved active antiseismic system using an auxiliary interferometer to make seismic motions of the suspension points at opposite ends of each arm track one another.
- (4) Wideband optical recycling is employed to increase effective light power.
- (5) Broadband operation is envisaged, with useful sensitivity over the range from below 100 Hz to above 5 kHz.

(B) Base Model, Version 2 (Narrowband)

Almost all main components are identical to those of Version 1, but some of the internal optics are modified to give optical resonating (Section V-A.2b) for optimized narrowband searches.

(C) Upgrade 1

Either version as above, or with Upgrades 2 or 4, but with light power increased to 20 watts by use of four argon lasers with their outputs added together coherently. This would be expected to improve sensitivity by a factor of 2 at the higher frequencies.

(D) Upgrade 2

Addition of active antiseismic guard system along three axes of the test masses near the junction of the arms, and along the transverse and vertical axes of the test masses at the remote ends of the arms. This can be applied to any of the versions or upgrades.

(E) Upgrade 3

Replacement of the argon laser light source by a Nd:YAG laser system with frequency doubler giving 100 watts of stabilized green light. This would be expected to improve sensitivity over that of Upgrade 1 by a factor slightly more than 2 in the high frequency region, and reduce electric power consumed.

(F) Upgrade 4

Increase the size of the test masses to 1 ton by bonding the smaller test masses with their low-loss mirror coatings to the front of larger fused silica masses, using optical contacting. This is a modification which may extend low frequency performance at some possible penalty in high frequency performance, so is more likely to be used as another concurrently-operating receiver than as a change to the Base Model.

(G) Upgrade 5

Use of squeezed-light techniques (Section V-A.2b). A probably late addition to improve performance of the broad-band model receivers.

Two possible Downgrades have been considered:

(H) Downgrade 1

The Base Model, Version 1, without recycling.

(I) Downgrade 2

The Base Model without the slaved active antiseismic system.

F.4 Specific Aspects of the Receiver Design

This complete receiver design is an integrated whole, with the optical interferometer section, the laser light source, a beam conditioning system, and the test mass suspension with servos for controlling test mass position and orientation, tightly integrated together and most of them influencing one another. The design in fact encompasses a family of variants of the basic system but some idea of the general philosophy may be gained from just two diagrams, Figure F-1 (placed following page F-10 for convenient reference while reading the explanation) which shows the main optical layout and some of the interferometer servos, and Figure F-2 (on page F-12) which indicates schematically how the suspensions and the positions of each of the four test masses are controlled.

To clarify the operation of the system, the diagrams are simplified to a considerable extent, and details such as lenses, amplifiers etc. are omitted.

(A) Main Interferometer (Base Model)

The main interferometer is based largely on the present 40-meter prototype and on experience obtained with this instrument. By designing the Base Model system for operation by a single argon ion laser, giving an input of only about 6 watts, it has been possible to make the design a very conservative one, with no components transmitting unusually high powers, and no requirement for any Pockels cell or other electro-optic or acousto-optic modulators any larger than those already used in the prototype. Indeed no components are exceptionally large, and even the main Fabry-Perot mirrors (8 inches in outside diameter, with a 5.5 inches diameter working area) do not require a figure accuracy any better than that of normal good optical components—as will be discussed later. In spite of the low input power and low power rating required of active components, high sensitivity is achieved by a recycling technique.

This receiver design includes several new features and concepts, not previously described, so we outline the operation of the system in stages in spite of the interconnections. It is simplest to begin with the basic interferometer, shown on the right hand side of Figure F-1 (following page F-10), and proceed gradually backwards through the system to the lasers on the left.

(1) Interferometer

The two main interferometer cavities, spanning the 4 km arms of the system, are shown at the extreme right-hand side and top of the Figure, labelled C2 and C1, respectively. The main beamsplitter, made with a heavy fused-quartz substrate suspended like the test masses and rotated by 45 degrees, is apparent between the cavities, along with

a matched compensating plate of fused quartz suspended parallel to it in the beam to the upper cavity.

Light enters and leaves the interferometer through two rather large additional cavities, C0 to the left of the beam splitter in the diagram and C3 below it. Both are formed by low-loss mirrors on heavy fused-quartz substrates, almost identical to the main test masses and suspended in the same way, and each cavity is about 10 meters long. The cavity C0 acts partly as a mode-cleaning cavity, and also performs other important functions in the system, while the cavity C3 is an output filter protecting the main output photodiode D1 from possible sources of spurious light such as scattered light from the walls of the 4 km beam pipes.

The central interferometer has some special features. The beamsplitter is made with a wedge angle of about 5 degrees, and its back surface has an antireflection coating designed to reflect 1% of the light from that surface, to a Pockels cell P1, which provides the main internal phase modulation for the interferometer. A mirror M returns light back to the system through the Pockels cell. The placing of the main modulator in a side arm of the system in this way has important advantages: it keeps the cell out of the high-power beam, reducing losses and possible radiation damage in a recycling system, and it makes it practical to add a small telescopic lens system (not shown) to reduce the beam size in the Pockels cell crystal from the diameter of 2 inches used for the 4 km beams to around 3 millimeters so that the small Pockels cell currently used in our prototype interferometers will be large enough. Thus the use of special high-power or large-size components is avoided.

If we omit recycling at this point for clarity, the primary locking system for this basic interferometer involves two separate frequency-locking conditions: the cavity C1 is made to resonate with the light from the laser source and the cavities C2 and C1 are brought into precise resonance with one another. The locking technique used here (and in many other places in the system) is our now-standard radiofrequency reflection locking method [F-1]. Frequency modulation at 12 MHz by the Pockels cell P1 is used for both functions. The locking into resonance of cavity C1 is done by coherently demodulating the signal from auxiliary photodiode D2 and using this to move appropriately the suspension point of the end test mass of this cavity by a coil-magnet system. (At this point the laser light is already well stabilized in frequency by a separate long-term-stable reference cavity, assisted at high frequencies by some feedback from the high-frequency-stable mode cleaner cavity, so a narrow bandwidth low-power feedback loop is adequate.) The main locking of cavities C1 and C2 together is done with much wider bandwidth and precision, using the full light power in the system, with diode D1. (In practice, with the system shown, an auxiliary narrow-bandwidth servo system is used to maintain the correct position for mirror M. This servo has been omitted for clarity, but it utilizes low-frequency (about 10 Hz) dithering of the mirror position to optimize the 12 MHz modulation amplitude, a technique used elsewhere in the receiver when a low bandwidth servo is sufficient to maintain just the steady position of a component.)

This outline covers in a basic way the primary locking of the main interferometer, but in the actual full system some further locking or stabilizing conditions have to be achieved. In particular it is necessary to ensure that the distance between the input

mirrors on the cavities C1 and C2 and the beamsplitter are kept such that a maximally dark fringe is obtained at photodiode D1 when both these cavities are in resonance, and also that the auxiliary cavities C0 and C3 are kept in resonance. There are several ways of achieving the first condition. One of these, as suggested in Figure VI-1 involves maintaining both main cavities in resonance independently of holding a dark fringe at photodiode D1; and here this may be done by locking cavity C1 as monitored by light reflected from the compensating plate, by adjustment of the position of its input mirror. The mode cleaner cavity C0, is locked to the input laser beam by phase modulating the input light to that cavity at 12 MHz, and using reflection locking with diode D6. Locking of C3 is done in the same way, using 30 MHz phase modulation applied to the input light after the cavity C0. In this interferometer design, it is planned to control the alignment of the mirrors in all of the optical cavities by the wavefront-phase type of automatic alignment system developed on the 40-m prototype, outlined in Section VI.A.1(d). In this diagram the complete automatic alignment system for one cavity, including quadrant diodes and lenses and associated electronics, is indicated by the square symbol containing the letters AA. Thus cavity C2 is kept in alignment by the Auto-Alignment unit directly below it, C1 by the unit to its left, etc.

(a) Recycling Control

The description above does not take recycling into account, but this is a relatively straightforward addition [F-2]. A special mirror assembly, labelled R, is used for recycling. Pockels cell P2 is used to apply an additional 14 MHz phase modulation to the main beam, which is then picked out by the photodiode D4 and used to lock the recycling mirror in the position for optimum operation. To avoid any loss in amplitude of the 30 MHz phase modulation in the recycling mode the free spectral range of the internal cavity formed between the recycling mirror and the input mirrors for cavities C1 and C2 is made to be a multiple of the 30 MHz modulation frequency, so that there is buildup of the sidebands as well as of the primary beam.

Acquisition of recycling condition is aided by use of a variable reflectivity mirror for R. One way of doing this is to have two close mirrors, separated by piezo transducers, so that the small cavity between them can be easily brought into resonance or out of resonance, thus changing transmission of the pair, and altering effective reflectivity. (Other ways of achieving this aim are possible, including use of frustrated internal reflection, tested earlier, or a commercial variable polarization beamsplitting unit.)

(b) A Technique for Compensating Errors in Mirror Figure and other Sources of Wavefront Distortion in a Recycling Interferometer

A technique is proposed here for much reducing demands on the figure accuracy of the super-polished mirrors which had earlier been thought necessary for good recycling. We propose the mirrors are made with only normal accuracy (of order one tenth wave). Then the compensator plate is manually hand figured while set up in an interferometer test rig using the actual components made for the real system, so that the hand-figured plate can correct for the sum of the errors in all the other parts. This is significantly easier since the compensating plate has no need for super polish, and only one surface has to be worked on for the whole system. It may be noted also that as the compensating

plate (of refractive index n) operates in transmission rather than as a mirror defining the wavefront of a nearly-Gaussian beam the effect on the optical path of a given dimensional error is reduced by a factor of approximately $n/(n - 1)$ for normal incidence, which is nearly 3 for fused quartz, and by an even larger factor at Brewster's angle. Thus the compensating plate has much less critical demands on figure accuracy than the surfaces of the cavity mirrors. The whole approach looks a very practical one. We have been told by a manufacturer of large high-precision optics who is involved in work on our prototype 40-m test masses that the required accuracy is normal practice with hand figuring, and over larger areas than ours. (It is expected that static wavefront correction will be entirely adequate, but if necessary a small additional dynamic phase correction can be applied by other techniques.)

Having now outlined the basic interferometer, we proceed to the functions and operation of the input mode cleaner C0.

(B) Beam Conditioning System

Light from the laser source enters the interferometer from the left, near the upper center of the figure, by a path labelled "from laser". The system begins with a rather large mode cleaning cavity C0, formed by concave low-loss high-reflectivity mirrors made on separate heavy fused-quartz substrates almost identical to the main test masses of the detector, and suspended and seismically isolated in vacuum in a similar but simplified way.

This cavity plays an important role in achieving high sensitivity in the interferometer, for it can define the direction of the primary laser beam with extremely high stability in the gravity-wave frequency range (50 Hz to 5 kHz). Our target here is transverse beam position fluctuations at 4 km distance of order 1 micron over this frequency range. Achievement of this stability is not in any way essential, but it is expected to be fairly easily reached by using suspension and damping techniques for the mode cleaner mirrors similar to those used for the main test masses, and this will make the interferometer relatively insensitive to small-scale surface figure errors and certain scattering phenomena in the main mirrors.

The mode cleaner mirrors are from 5 to 10 meters apart, and weigh about 8 kg. At this separation the spot size on the mirrors is large enough to make mirror distortion due to heating insignificant at the planned input power levels. The optical bandwidth of a cavity of this size made with mirrors similar to those in the 40-m prototype can be made 5 kHz or lower without significant attenuation, and this enables the cavity to fulfill another important function: additional filtering of the input beam against fast frequency, phase and intensity fluctuations. Experience with the 40-m prototype has shown that high-frequency noise in the laser can produce troublesome intermodulation phenomena in the photodiode or electronic systems, and a mode cleaner can filter out several types of spurious effects occurring in the lasers of the gravity-wave detector.

In this receiver design the beam arrives at the mode cleaner from the laser system already well frequency stabilized to a separate highly-stable reference cavity at frequencies up to at least 5 kHz. The mode cleaner has its length controlled by a magnetic force-feedback system to lock it into resonance with the laser beam, using our standard

radiofrequency reflection-locking technique. Phase modulation is applied to the input beam at 12 MHz, by a Pockels cell (labelled PC) in front of the cavity; and the reflected light, separated from the main beam by a quarter-wave plate and a polarizing beamsplitter, is detected by photodiode D6.

This mode cleaning cavity, with its well-isolated and heavy mirrors, can provide an extremely quiet final frequency reference for the laser beam, at all but low frequencies. In this design it is used as a second stage of laser frequency stabilization, by feedback of high-frequency components in the error signal to an additional phase-adjusting Pockels cell in the input beam.

The beam continues via a further phase-modulating Pockels cell, polarizing beamsplitter, and Faraday rotator (FR) to the main interferometer.

(C) Beam Generating and Control System

(1) Base Model—Single Laser Source

The Base Model receiver uses as its light source a single argon laser in a two-stage frequency stabilization system, with primary stabilization to a special high-mechanical-Q reference cavity, and a secondary trim for fast frequency fluctuations controlled by the mode cleaning cavity of the interferometer. Figure F-1 shows two lasers to indicate the overall concept. In the single-laser Base Model the laser would be arranged as shown by the laser at the extreme left-hand side of the Figure—labelled as Laser 1—and the laser shown to the right of this would be omitted.

The laser frequency is controlled by fast, small-range, and slow, large-range, piezo-driven mirrors at opposite ends of the laser cavity, aided by a wide-bandwidth trim of output light phase by a series Pockels cell [F-3]. Thus the laser cavity is kept free of electro-optical components which might limit available power or be affected by U.V. radiation damage. The laser beam passes via an isolating Faraday rotator (FR), the phase-trimming Pockels cell, an electro-optical amplitude modulator, and a radio-frequency phase modulating Pockels cell to the high-Q reference cavity C4. This reference cavity is constructed from a drilled bar of fused quartz, with end mirrors optically contacted to the ends, and is suspended in vacuum by wires from seismically isolated supports using techniques similar to those developed for suspending the bars of room-temperature resonant bar gravity-wave detectors. This gives very low mechanical and thermal noise. An automatic alignment unit (AA) aligns the laser beam to this quiet cavity by servo-driven mirrors, thus providing a first stage of active beam direction stabilization and beam wiggle reduction. An intensity monitor photodiode D9 controls the amplitude modulator, to stabilize output intensity. The stabilized output beam then passes via a second phase-trimming Pockels cell (near the center of the Figure) and a second pair of direction-controlling and position-controlling servo mirrors to the mode-cleaning cavity C0 of the main interferometer. This second phase-trimming Pockels cell receives control signals covering frequencies from about 20 Hz upwards from the mode-cleaning cavity, to give a second wide-band high-gain frequency stabilization loop based on the even quieter high-frequency reference given by the heavy isolated masses and mirrors of the mode cleaner. The complete two-stage frequency and direction stabilization system is designed to give a final beam suitable for the main interferometer without requiring any

frequency control from the 4-kilometer arms, thus avoiding any possible complications from kilometer propagation delays or the small free spectral range of the 4-kilometer cavities.

In the diagram each set of servo-driven mirrors used for controlling beam direction and position are indicated as a pair of mirrors. In fact separate fast small-range mirrors and slower wide-range mirrors are employed, to give a good combination of dynamic range and speed of response, and using four mirrors per set. Further stabilization of beam direction and position extending to the highest frequencies is provided passively by the mode cleaner C0. The dimensions of the mode cleaner cavity are determined in part by possible thermal effects in the mirrors at high intensities, and as well as by considerations of directional stability. For the power level of the Base Model receiver a cavity 0.5 meter long could be adequate, but for the higher power levels of the proposed receiver upgrades a cavity of length of about ten meters is envisaged; and as this will also give better directional stability this size is chosen for the Base Model design.

The schematic diagrams given show only one of a large number of possible design variants, and are intended to illustrate more the general approach than the final details. In this laser stabilization system, for example, it may prove useful to supplement the Pockels cell phase shifter shown in the first loop by an acousto-optic frequency shifter; or it may be useful to feed back a trimming signal from the second stage stabilizing loop to the first one. Current work with prototype interferometers is giving practical experience of these and other variants of the basic stabilization system. The arrangement shown in the figures is a fairly straightforward one, and a reasonable choice for the present design.

(2) Upgrade 1—Coherently-Added Multiple Laser Source

To upgrade the receiver it is proposed that light power be increased by adding coherently the outputs from several lasers, and use of four lasers is envisaged as Upgrade 1. The light frequency is determined by a single primary laser, and additional "booster" lasers are phase locked to the output of the primary laser and added coherently to it.

The primary laser system is identical to the Base Model laser system described above, and this defines the initial frequency and directional characteristics of the output beam. Each booster laser has its frequency, phase, and beam direction slaved to that of the primary laser, as is shown for one typical secondary laser (labelled laser 2,3,4), to the right of the initial laser 1, in Figure F-1. The beam from this secondary laser, after intensity and directional stabilization, passes to a beamsplitter which adds its output coherently to the output beam from the previous laser (or lasers) to contribute to the total output directed towards the interferometer. By monitoring the output from the other side of this combining beamsplitter with photodiode D6, a signal is obtained which is used to stabilize and phase lock the secondary laser to the output of the first. For efficient operation of this combining system the reflectivity of the combining beamsplitter has to have a specific value which minimizes the light rejected downward. The simple beamsplitter shown in the diagram is only to indicate the principle; in practice an adjustable beamsplitting system is used, and in fact an automatic self optimizing combining system has been designed to cope with changing laser outputs.

In the complete system, with one primary laser and three secondary ones, the secondary lasers use different modulation frequencies to avoid possible interaction, and the combining beamsplitters for each have different reflectivities unless adjusted automatically. The optical configurations for the three secondary lasers are otherwise identical.

Reliable coherent addition of a number of argon lasers requires that the single mode etalons used in each laser to select the operating longitudinal mode must be adjusted to select modes close in frequency to one another—at least to within about one free spectral range. Commercial lasers are designed so that the etalon is sufficiently stable for initial manual adjustment to be adequate, and this may be adequate for this system also. However the receiver design has provision for an auxiliary control system for controlling the resonant frequency of the single mode etalon in each laser.

The multiple laser source system outlined here can be extended to larger numbers of argon lasers. At a certain point it will probably become economical to switch to a more efficient type of laser system, such as a Nd:YAG laser with frequency doubler. For high power levels the system can consist of a low power laser oscillator, followed by a laser amplifier and a frequency doubler, and in this case a stabilization system similar in principle to that for the Base Model may be suitable for controlling the oscillator stage. The wavelength of the light from a doubled Nd:YAG system (530 nm) is sufficiently close to the wavelength of the green line from the argon lasers used in the design here (514 nm) that this switch of laser type can be made with minimal changes to the rest of the receiver system, when suitable laser systems become available. In this design this switch is suggested as Upgrade 3. The basic design outlined here seems capable of extension to much higher power levels than proposed for initial use, with corresponding long-term advances in ultimate performance.

(D) Test Mass Control and Isolation System

(1) Base and Upgraded Models

The primary isolation for the Base Model design is passive, and the main mass suspension inside the vacuum enclosure is in essence identical to that already well established in the 40-meter prototype. Experimental studies with the prototype system have indicated that at the proposed interferometer sites it will almost certainly give by itself more than adequate isolation against direct seismic noise at all frequencies above about 100 Hz. A major part of the isolation here is given by five-layer lead and rubber stacks, and the only changes are to improve high-vacuum compatibility by encapsulating the individual rubber pads in very compliant sealed metal bellows and by replacing the layers of lead by layers of stainless steel. As in the present 40-meter system, the design has provision for air suspensions outside the vacuum system to assist in low frequency isolation.

Arrangements for damping the seismic pendulum motions of the test masses in the Base Model are essentially similar to those already used in the 40-meter prototype or currently being installed there. To improve low frequency isolation auxiliary interferometers, as currently being installed in the prototype, are arranged to monitor differential motions of the mass suspension points along each arm. These operate servo systems

designed to make the suspension points at the stations distant from the central station track motions of the central ones.

In the Base Model version the four test masses have certain of their pendulum degrees of freedom damped to their local mounting baseplates (on the isolation stacks), using LED/photodiode shadow sensors to monitor relative motion, with piezoelectric feedback to the suspension blocks for motions in the direction of the arm—as in the prototype. Some additional vertical compliance in the suspension will be introduced by incorporating a spring in the wire supporting each suspension block, and vertical and horizontal motions of the mass transverse to the beam direction are also monitored, and horizontal and vertical damping provided by magnetic feedback to the block.

In the Upgraded Model the shadow sensors are replaced by active guard feedback systems, which cause the suspension points to track the test masses below them. This active isolation is applied to different sets of axes for the master and slave test masses. The arrangement is shown in Figure F-2, with the full feedback shown for only one of the two arms, for clarity. Both arms are similar. (It may be noted that the horizontal isolation system used here uses reference arms, as developed in early work at Glasgow [F-4], and the vertical feedback system used is equivalent to the “super spring” system developed at JILA [F-5].

An important feature of the design is that the four test mass suspensions are not operated as independent units. One test mass is regarded as the “master” mass—(labelled A in Figure F-2)—and this is taken to define an effective inertial frame for the whole system, for motions in the directions of the main beams. The suspension points for the other masses are slaved to this master one using signals provided by the main and seismic suspension point interferometers, aided at low frequencies by additional beam position monitors (not shown). Relevant degrees of freedom of each test mass suspension are controlled as follows:

Mass A. The Master mass. Free for translational motion in longitudinal, horizontal, and vertical directions—aided in the Upgraded model by the active guard system or in the Base model controlled at low frequencies by damping to local ground. (Rotational degrees of freedom for this and the other masses are separately controlled by the automatic alignment system outlined earlier.)

Mass B. A Slave mass. Longitudinal motion of the suspension block forced to track motion of the suspension block for mass A, using the seismic monitor interferometer. Transverse motions of the mass in horizontal and vertical directions made free by active guard system (Upgraded model) or damped at low frequencies to local ground (Base model).

Mass C. The “Secondary Master” mass. Similar to mass A, but very-low-frequency components (0 to 1 Hz approximately) of vertical and transverse mass position forced to track position of main interferometer beam, using signals from additional monitors.

Mass D. A Slave mass. Control of suspension block similar to that of slave mass B, with longitudinal position slaved to mass C by the seismic monitor interferometer. However there is an additional high-precision wide-band control of the longitudinal position of the mass to make the main interferometer arms very closely equal (plus

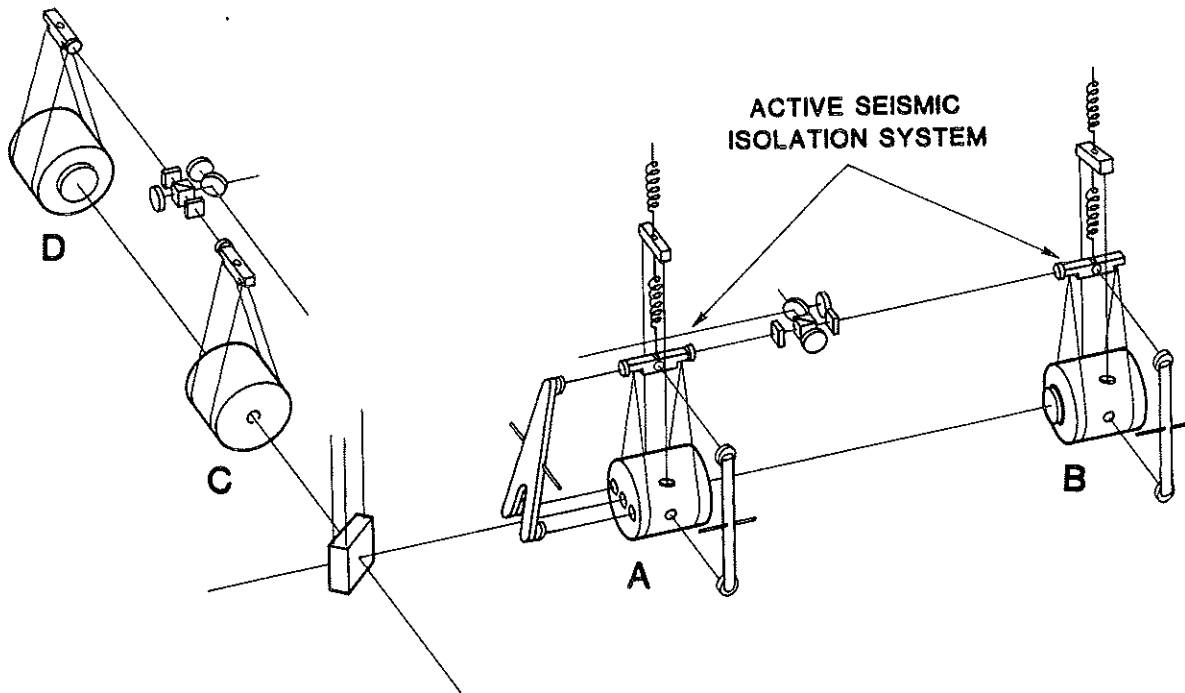


Figure F-2 Simplified sketch of arrangement of test mass suspensions in Upgrade 2 of a Fabry-Perot receiver for the LIGO, showing an active antiseismic guard system for test masses A and B added to the slaved antiseismic system of the Base Model. The suspension block of the Master test mass A is driven to track longitudinal and transverse motions of the mass using auxiliary interferometers monitoring distances to upper and lower ends of freely pivoted reference arms which remain stationary. The upper support piece, from which the main suspension block hangs by a spring, is driven to track vertical motions of the test mass, using vertical monitoring laser beams. Control of transverse and vertical motions of the effective suspension points of slave mass B is similar, but its longitudinal position is driven to track that of master mass A by the seismic monitor interferometer. The guard system for test masses C and D are similar to those for A and B, respectively, but for simplicity are not shown here.

or minus an integral number of half-wavelengths) by direct electrostatic force applied to the mass itself from a capacitor plate on a separately suspended recoil mass, using signals from the main interferometer.

(a) Note on the frequency stability of the seismic monitor laser source

The seismic monitoring suspension point interferometer on the 40-meter prototype (Figure VI-10) uses a normal helium neon laser stabilized by thermal and piezoelectric feedback to a length of optical fiber. This simple system was chosen for convenience, and could be used in the large system with some additional feedback from one of the arms: as the two arms use the same light source, frequency fluctuations cancel. However in the 4 km design, a by-product from the main interferometer system is a very highly stabilized laser source (stable to about a part in 10^{14} in the relevant low frequency region). In this design, a few milliwatts of this laser output is used for the seismic monitor, with its frequency shifted by 40 MHz in an acousto-optic modulator to avoid any danger that scattered light could affect the main interferometer system.

(b) Additional details of the seismic monitor system

The present 40-meter prototype uses a single-bounce unequal-arm Michelson interferometer for the seismic suspension point monitor of a single arm. Higher performance with low light consumption can be achieved with Fabry-Perot cavities in each arm. To keep the size and weight of the mirrors attached to the suspension blocks small, the present design (like the 40-meter prototype) uses lenses in a cats-eye retroreflector system with the lenses supported independently of the suspension blocks, in this case from the isolated baseplates.

(E) Automatic Beam Alignment and Control System

The units marked AA in Figure F-1 are automatic alignment systems which match wavefront phase, similar to the original prototype unit at Caltech. The action of this unit is effectively an extension of our old laser phase-locking technique to the spatial domain, and it uses the same basic radio-frequency techniques, mostly here with the same 12 MHz modulation frequency as the cavity and laser locking systems. A pair of quadrant photodiodes arranged to sample cross-sections of the reflected beam from a cavity at different distances along the beam sense transverse gradients of phase difference between the stored light from within the cavity and the input light reflected from the input cavity mirror, and generate control signals which tend to drive these phase difference gradients to zero. Like the phase-locking technique, this system uses light efficiently, has good signal to noise ratio, and can have wide bandwidth—up to about 1 MHz.

In the complete system, additional monitors of beam position are required, but these are omitted from the diagram for clarity.

To follow the operation of the complete aligning system it should be realized that the AA units can be made either to lock a laser beam along the correct common optic axis of a pair of fixed cavity mirrors (even though this axis may not pass through the center of either mirror), or to lock a pair of cavity mirrors into correct orientation with a fixed laser beam—in each case with wide bandwidth.

In the complete interferometer design, the master mass A and the slave mass B define the main optical alignment of the whole system. The main resonant beam in cavity C2 is arranged to pass through the centers of the mirrors on the test masses A and B by adjustment of the axis of the mode cleaner, either manually or by an auxiliary slow control system (not shown). The AA unit directly below cavity C2 in the diagram sets the orientation of the masses accordingly. Thus these two nearly inertial test masses determine the alignment and transverse location of the whole beam, running right from the center of the Figure. In the second arm of the interferometer, one end of the input beam is forced to meet the now-fixed primary beam (at the beamsplitter), and the other end of the beam is defined by the position of the center of the mirror on test mass D, to which it is directed by adjustment of the orientation of the beamsplitter. Again, this adjustment may be done either manually or by an auxiliary slow control system.

Similar actions are repeated throughout the interferometer. Some parts of the automatic control system in this design perform several of the functions previously done by optical fiber in prototypes, in allowing some independence and even relative motion between the positions of the laser system and the interferometer, and providing

some (slow) beam-dewiggling action. However this system proposed here ensures that correct alignment is maintained entirely automatically, and it can handle much higher powers than a fiber system with presently-available fibers.

Finally, the filtering cavity for the output photodiode is aligned by its own AA unit.

A system of the type proposed here should be much more user-friendly than any of the prototype gravity-wave interferometers, and capable of both reaching much more precise alignment than a manual system, and maintaining it for long periods. A manual alignment system is still required for initial start up, and in this design we propose use of a computer- controlled switching system to keep the manual system monitoring and adjusting its own alignment during normal automatic operation, but giving switch over to the manual system in event of loss of lock or other automatic-system failure. On recovery of lock, the system would switch itself back to automatic operation, giving minimum disturbance. This system will be very similar to the one currently being set up for initial tests on the 40-meter prototype with an IBM PC as a simple control computer.

An automatic alignment system is an essential feature for a 4 km interferometer, and the Fabry-Perot cavity autoalignment device already demonstrated on one arm of the 40-meter prototype provides a very precise and drift-free way of achieving this, as indicated in this design. The system may appear slightly complex overall, but it should be noted that it is made up mainly of many identical copies of a few basic units which will be designed to be suitable for small-scale quantity production.

The simplified schematic diagram given shows only one of a large number of possible design variants, and is intended to illustrate more the general approach than the final details. In this laser stabilization system, for example, it may prove useful to supplement the Pockels cell phase shifter shown in the first loop by an acousto- optic frequency shifter; or it may be useful to feed back a trimming signal from the second stage stabilizing loop to the first one. Current work with prototype interferometers is giving practical experience of these and other variants of the basic stabilization system. The arrangement shown in the figures is a fairly straightforward one, and a reasonable choice for the present design.

References

- F-1 R. W. P. Drever, J. L. Hall, F. V. Kowalski, J. R. Hough, G. M. Ford, A. J. Munley, H. Ward, *Applied Physics* **B31** (1983), 97.
- F-2 R. W. P. Drever, J. Hough, A. J. Munley, S.-A. Lee, R. Spero, S. E. Whitcomb, J. Pugh, G. Newton, B. Meers, E. Brooks III, Y. Gursel, "Gravitational wave detectors using laser interferometers and optical cavities: 1. Ideas, Principles, and Prospects" *Quantum Optics, Experimental Gravity, and Measurement Theory* ed. P Meystere and M. O. Scully, (Plenum Publishing, 1983), pp. 503-514.
- F-3 G. A. Kerr, N. A. Robertson, J. Hough, C. N. Man *Applied Physics* **B37** (1985), 11.
- F-4. N. A. Robertson, R. W. P. Drever, I. Kerr, J. Hough, *J. Phys. E, Sci. Instr.* **15** (1982), 1101-1105. J. Hough et al. "Gravitational wave detectors using laser interferometers and optical cavities: 2. Some practical aspects and results" *Quantum Optics, Experimental Gravity, and Measurement Theory* ed. P Meystere and M. O. Scully, (Plenum Publishing, 1983), 515.
- F-5 J. E. Faller, R. L. Rinker *Dimensions* (September 1979) p. 25.

Appendix G

PRELIMINARY DESIGN OF A LIGO DELAY LINE RECEIVER

This appendix presents two conceptual delay line receiver designs to meet the initial LIGO sensitivity goal (middle curves in Figures A-4a,b,c). The designs are derived in part from the experiences with the 1.5 meter prototype at MIT, the 30 meter system at the Max Planck Institute in Munich, and the Fabry-Perot systems at Caltech and Glasgow.

The "L" configuration

Figure G-1 shows a schematic diagram of a LIGO delay line receiver in an "L" configuration which is similar to the 1.5 meter system. The light source is a 100 watt CW Nd:YAG laser operating at one micron. The input and output coupling of the interferometer is accomplished with single mode, large diameter optical fibers. The fiber ends are melted into lenses which, along with weak auxiliary lenses, mode match to the optical cavities. Each coupler is mounted on a separately suspended and servo damped mass. The input beam is divided by a symmetric dielectric coated beam splitter mounted on a multiple isolated mass. The beams enter the two orthogonal delay line cavities through the input holes in silicon substrate mirrors. The mirrors have multilayer dielectric coatings on their curved surfaces and are polished on their flat surfaces. The beams in each cavity bounce back and forth between the mirrors making a circular pattern of spots on the mirrors. The spots are separated so that the intensities incident on the mirror coatings are minimized. The design is configured for 34 passes* of the beam in each cavity (a storage time of 0.5 milliseconds) before the beams emerge through the output holes in the mirrors. The position and rotation of each mirror is controlled electrostatically relative to a suspended guard mass (not shown) in a multiple suspension system. On exiting the cavities, the beams pass through Brewster angle longitudinal electrooptic phase modulators driven by RF in antiphase to impress sidebands on the optical carriers for subsequent fringe interrogation. The two electrooptic crystals are mounted together on a separately suspended mass. The phase modulators are also used as phase controllers in a servo fringe locking system with large bandwidth but small dynamic range. Large dynamic range, lower bandwidth fringe control is asserted by electrostatic controllers on the mirrors. The beams are recombined on a separate beam splitter which is identical in construction to the input splitter. Both the symmetric and antisymmetric outputs are coupled out of the interferometer to high power photodetectors. The figure does not show the auxiliary light beams and area detectors used for mirror pointing or the separate low power interferometers that control the relative positions of the the two input mirrors and the beam splitters.

* Figures G-1 and G-3 refer to a 36-pass delay line, but the 34-pass geometry is preferable because of differences in the spacing of the spots on the mirrors. The curves in Figure 3 are only slightly different for a 34-pass geometry.

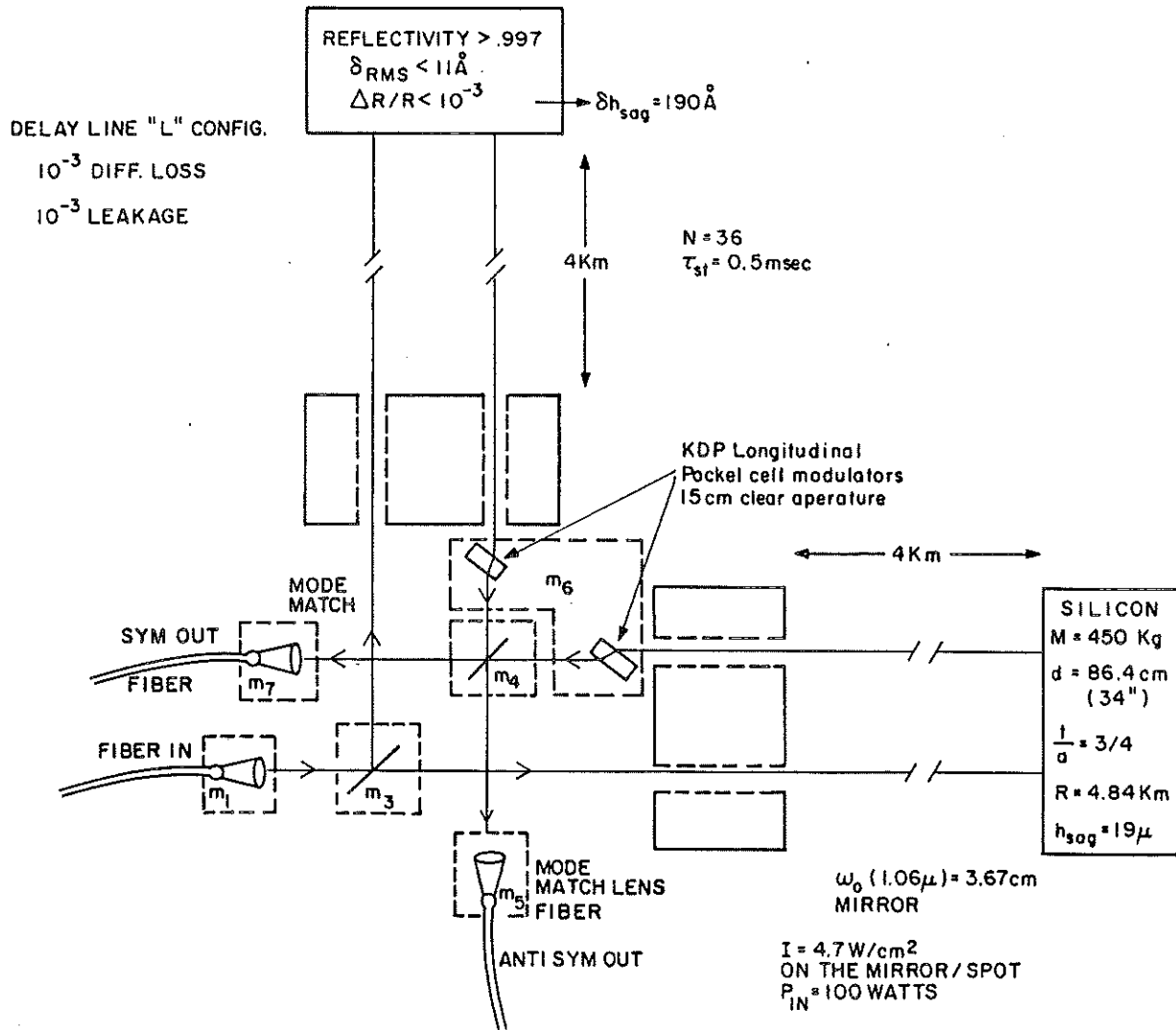


Figure G-1: Schematic diagram of a LIGO delay line receiver in an L configuration.

Positive attributes of the design

The principal advantage of the design is its simplicity and minimization of optical components in the transmission path that can distort wavefronts and scatter light. The mirrors can be monolithic and do not have to be transparent so that an optimized tradeoff of such material properties as substrate mechanical Q, thermal expansion, and the quality of the polished surface can be made over a large range of materials. The delay line interferometer is operated on or near the "white light" fringe so that laser frequency stabilization is not required except as one means of controlling the fringe noise of scattered beams from stationary scatterers and to relax the requirement of strict path length equality. Control of noise from scattering uses the technique of reducing the coherence length of the light by random phase modulation, which is effective for both stationary and moving scatterers. The method is easier to implement in a four

kilometer system than the 1.5 meter system since the time delays between the main beam and the principal scattered beams, originating from different spots on the mirrors, are larger. Beam jitter is controlled by the optical fiber coupling at the input and scattered fields other than those that overlap with the mode defined by the exit output fibers are rejected. This serves not only to reduce the total scattered intensity but also to relax the demands on the uniformity of the photodetector. The fringe phase is, in first order, nearly insensitive to translation of the mirror perpendicular to the optic axis as well as to mirror rotation. This is most strictly true for a completely reentrant geometry, one in which the input and output beams are coupled through the same hole in the mirror. In a four kilometer system the two beams in such a configuration would be separated by an angle of 100 microradians so that auxiliary optics placed in the main beam would be required. The choice made in the design is to use two coupling holes at the cost of a small first order sensitivity to rotation and translation in order to avoid additional components. The relative ease of alignment of the system is preserved. Another possible attribute is that since the beams do not interfere in the cavity, effects associated with the "spring constant" of the optical field are unimportant. The requirements for the vacuum system are relaxed since the amplitude of optical phase fluctuations due to fluctuations in the column density of the residual gas in the cavities is reduced relative to a single beam interferometer in the ratio of the square root of the number of beams.

Developmental requirements and disadvantages of the design

The delay line receiver requires additional development of mirrors of the size and surface quality shown in Figure G-1, modestly large aperture electrooptic crystals, and high power optical fibers and lasers. There is a tight constraint upon the mirror curvature error driven by the need to satisfy simultaneously the geometric constraint that the beam exit through the exit aperture as well as the requirement of optical path length equality in the two arms. The use of two independently suspended beam splitters relaxes this constraint slightly. Representatives of Kodak and Perkin-Elmer maintain that our requirements are less stringent than those of mirrors for surveillance satellites and the Space Telescope, and that mirrors can be made to our specifications. Kodak has experience with nearly flat, super-polished mirrors on this scale, and Perkin-Elmer has the capability to measure the quality of such mirrors. We are concerned that a mirror initially made to specification might deform during use as a result of gravity loading or thermal deformation under high intensity illumination. Thus, there are alternative strategies to meet the requirements of beam geometry and optical path length equality. One possibility is to servo the mirror radius electrostatically. A second is to include a small steering mirror in the delay line cavity. Such a mirror, which would reflect the beam only once, would be movable along the optical axis of the cavity to vary the optical path length and it would be steerable to achieve the beam geometry condition. A third possibility is to use the closed path geometry which is described below. None of these three ideas has been tested. The constraint on surface microroughness is a result of the requirement for low scattering at the mirror surface. Coatings of this quality are achievable; Battelle Northwest uses plasma deposition to coat substrates as large as one meter diameter for the military. Delay line receiver mirrors are large enough to serve as the interferometer masses. The ratio of thickness to radius is chosen to put

the frequency of the lowest order normal mode outside of the frequency band of the gravitational wave search.

The delay line receiver requires longitudinal Pockels cell phase modulators with 15 cm clear apertures. KDP crystals of even larger size are made and used at Lawrence Livermore Laboratory, but they have not been tested for this application. The optical uniformity of the crystals and the transparency and scattering amplitude of the transparent electrodes are critical concerns. The crystals are not required to withstand high optical intensities; the peak intensity is small since the beam diameter is large. Similarly, high intensity capability is not necessary in the Pockels cells used for scattering suppression and laser frequency servo, because these cells will be situated between the laser oscillator and the power amplifier, and only a low power beam will be incident upon them. If large aperture crystals are not suitable for the delay line receiver, then one might focus the beam into a smaller crystal, but that crystal must be able to withstand optical intensities greater than the damage threshold in crystals currently available. Alternatively, one might construct a large crystal with an array of smaller crystals.

Optical fibers of sufficiently large diameter have not yet been developed. We know that optical loss is lower at one micron than at 0.5 micron, so it should be possible to transmit 100 Watts, but fibers of larger diameter than we have now will be required. Nd:YAG lasers which can generate 100 Watts of single mode light do not exist at present, but the development of this laser is a major development item both within the LIGO project and in industry. It is likely that adequate lasers will soon be available. Light recycling is not shown in Figure G-1, and it would require development. There is no reason that light recycling could not be used in the delay line receiver, though it does demand a level of frequency stabilization which is not otherwise required to meet the initial design sensitivity goal of Figure G-3.

An intrinsic limitation of the delay line receiver is that the storage time cannot be increased by large factors. Small increases are possible through the use of non-circular spot geometries, which might be achieved through the use of either astigmatic mirrors or steering mirrors. Nevertheless, Fabry-Perot and tagged-beam receivers hold greater promise to enhance the storage time.

Closed geometry delay line concept

An alternative to the "L" configuration is the closed path delay line receiver shown in Figure G-2. The most significant advantage of this geometry is that it relaxes the constraint on mirror radius error. The equality of optical path length is automatically satisfied and the cavity lengths can be individually adjusted to satisfy the beam geometry condition. The closed path geometry has slightly enhanced sensitivity relative to the "L" configuration in the band above 100 Hz. This is due in part to the increased storage time, but also because the transfer function of the configuration is larger at midband frequencies at the expense of low frequency sensitivity. Nevertheless, the design is such that the performance at low frequencies is still dominated by stochastic forces rather than Poisson noise.

The principal disadvantage of the closed path geometry is the multiplicity of optical

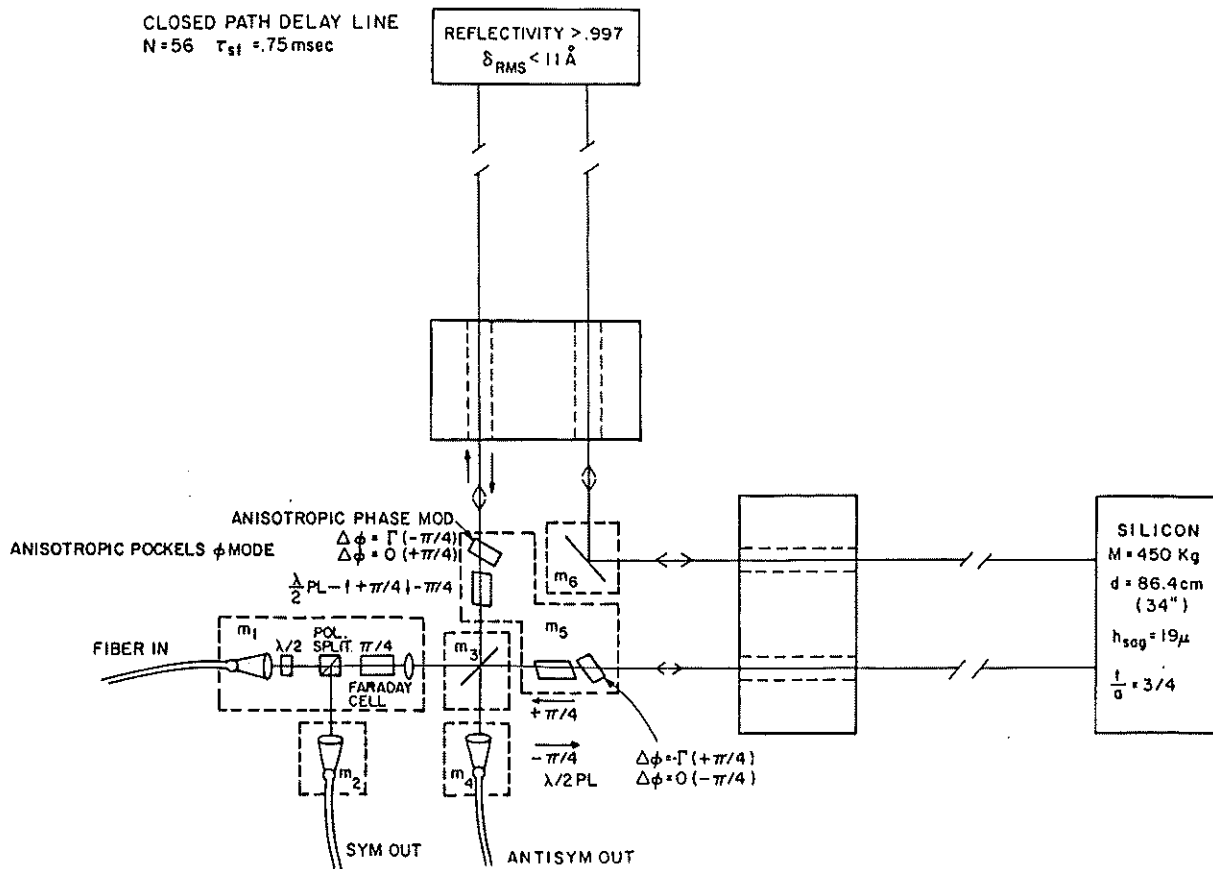


Figure G-2: Schematic diagram of a closed-path delay line receiver.

components required and their attendant losses and distortions. A minor disadvantage is the larger probability of backscatter from overlapping beam spots, though this is not serious as it is controlled by the reduced coherence of the light.

In the closed path design of Figure G-2 each beam traverses each cavity 28 times for a total of 56 passes and a storage time of 0.75 msec. Each beam passes through both Pockels cells, but a beam is modulated by only the Pockels cell through which it passes after having passed through both delay lines. Consider the beam which is reflected from the beam splitting surface on mass 3. Its plane of polarization has been rotated by $\pi/4$ by the Faraday cell, and it traverses the first Pockels cell perpendicular to the modulation axis of that cell, so no modulation results. After traversing one delay line, it is reflected by the mirror on mass 6 into the other delay line, and then passes through the other Pockels cell and is modulated. Similarly, the beam which is initially transmitted by the beam splitter on mass 3 is only modulated by the second Pockels cell through which it passes. The polarization states of the outgoing beams are such that they interfere at the beam splitter.

Proposed work on delay line receivers when and if reinitiated

Delay line research has been halted for the present time in favor of development

of Fabry-Perot receivers. If delay line receiver development is restarted, then efforts would be directed toward construction of an "L" configuration prototype receiver in the 5 meter vacuum system at MIT. Such a prototype would use mirrors of 8 inch diameter. Work on large aperture electrooptic modulators would have to be initiated. Some effort has gone into development of specifications for large mirrors; that work would have to continue along with the development of test methods for mirrors of large diameter and large radius of curvature.

Some development efforts are common to both Fabry-Perot and Michelson delay line systems. Work that is being carried out at present and which would be applicable to delay line receivers includes development of Nd:YAG lasers, large diameter optical fibers, and suspension systems.

Sensitivity of delay line receivers

Figure G-3 shows the anticipated strain sensitivity of an L configuration delay line receiver and a closed path receiver which are designed to meet the initial LIGO sensitivity goal. Seismic noise dominates the noise spectrum at low frequencies, thermal noise in the suspension is dominant at frequencies of roughly 50 to 100 hertz, and Poisson noise is the limiting noise source at higher frequencies. 100 watts of optical power is assumed.

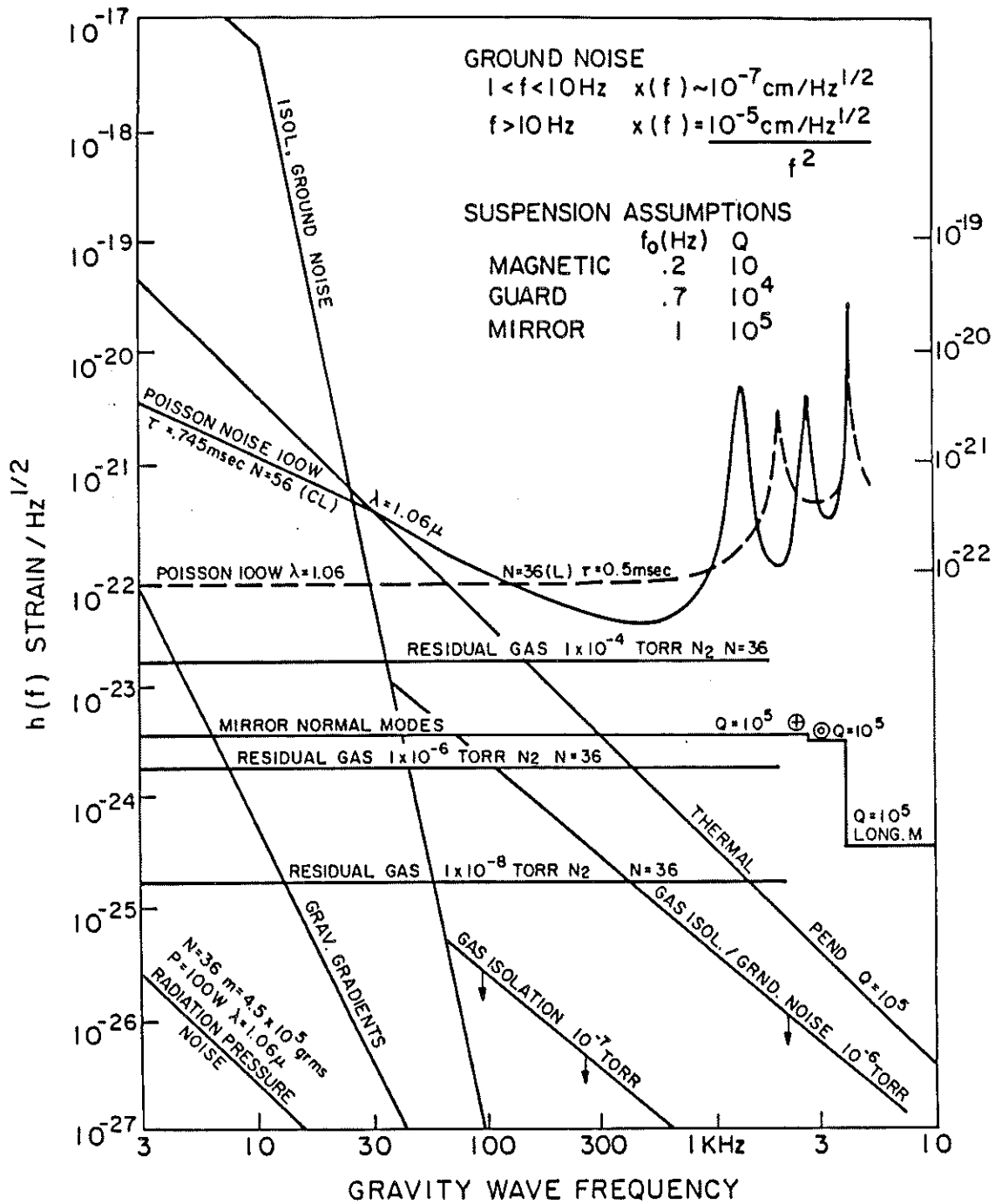


Figure G-3: Anticipated strain sensitivity of possible LIGO delay line receivers.

APPENDIX H

TECHNICAL DETAILS OF THE PROTOTYPE INTERFEROMETERS AND ASSOCIATED TECHNIQUES

H.1 Detailed Description of the 40-Meter Prototype

(a) The Technique to Maintain the Interferometer on Resonance

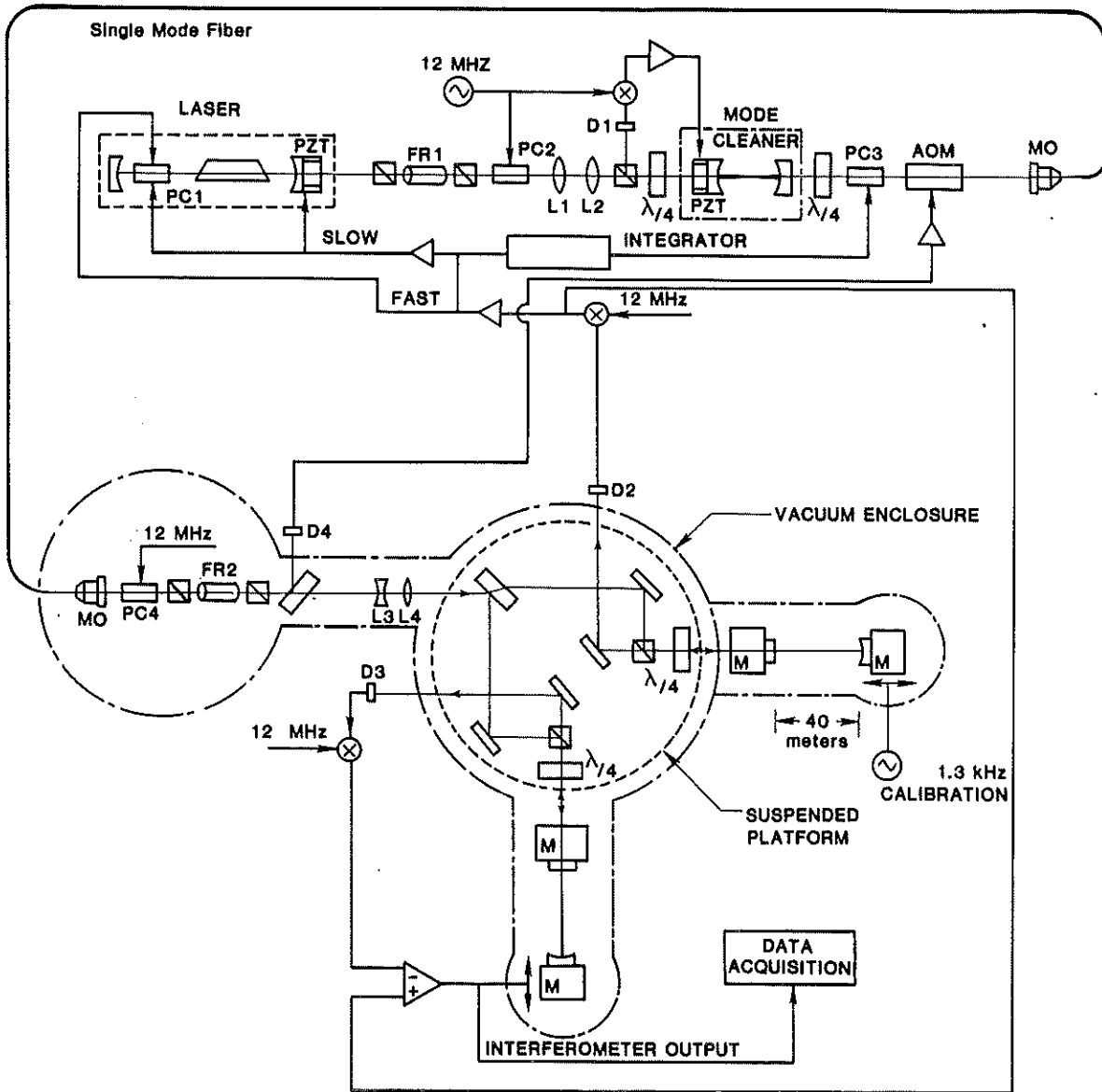
Figure H-1 shows schematically the optics and electronics of the 40-meter prototype interferometer, as of October 1987. An argon ion gas laser, tuned to 514 nm and operating in a single longitudinal mode, illuminates the interferometer. The fluctuations in laser wavelength and the low-frequency (below 10 Hz) motion of the suspended cavity mirrors are too large by far to maintain resonance without electronic feedback. The needed feedback signals are obtained by applying radio-frequency phase modulation to the input beam with Pockels cell PC4. The optical phase is modulated with an amplitude of approximately one radian at a frequency of 12 MHz. At this frequency laser intensity noise from turbulence in the forced flow of cooling water, plasma noise, and other spurious sources is negligible compared to fluctuations from photon counting statistics.

The modulated light passes through various components: a Faraday isolator to prevent stray back-reflections, a pair of lenses to match the beam to the cavity, and a beamsplitter. The split beam is steered into the pair of 40-meter cavities via directional couplers consisting of beam splitting polarizers and quarter-wave plates. The cavities exhibit an amplitude storage time of 0.5 milliseconds, which corresponds to a bandwidth of 300 Hz. Consequently they reject the 12 MHz sidebands, and the light striking photodiodes D2 and D3 is the vector sum of two components: the modulated beam from the laser reflected by the input mirror, and the cavity beam, without modulation sidebands which "leak" back out through the input mirror. In resonance, the laser and cavity beams have opposite phase, and the intensity on the photodiodes is a minimum. Due to scattering and absorption losses in the mirrors as well as imperfect matching of the input beams to the cavities, the minimum intensity is not zero, but rather 15% of the input intensity. If the mirror separation or the laser wavelength moves slightly away from the resonance condition, the 12 MHz component of the photocurrent in the detectors increases linearly. These error signals are demodulated by r.f. mixers coherently referenced to the same oscillator that applies the phase modulation to PC4.

The error signals from the two arms are fed back asymmetrically. The signal from D2 is applied to a set of controlling elements consisting of a Pockels Cell PC1 inside the laser, a piezoelectric transducer mounted on the laser front mirror, and the extra-laser phase-correcting Pockels cell, PC3. These correction paths combine to match the laser wavelength to the length of one arm, accurately maintaining resonance. The other arm is brought into resonance by mechanically adjusting its length, using the signal from photodiode D3 which is applied to transducers that move one of the end masses.

(b) Reduction of Spatial and Temporal Fluctuations in the Laser Beam

The Munich Group proposed [H-1] that small fluctuations in the geometry of the laser beam could be a source of noise and described a "mode cleaning" cavity to reduce



KEY TO SYMBOLS:














	Beam-splitting Polarizer		Piezo-electric transducer		rf demodulator (mixer)
	Pocket cell		Quarter-wave plate		Sine-wave generator
	Test Mass with mirror		Faraday rotator		Amplifier
	Mode-matching lenses		Acousto-Optic Modulator		Photodiode/amplifier
L1 - 4					MO Microscope objective

Figure H-1: Schematic diagram of the 40-meter system. Refer to text for details.

the fluctuations. Subsequently, an alternative method for spatially filtering the beam by passing it through a single-mode optical fiber was suggested by the MIT Group.

Both techniques are used in the 40-meter prototype: the beam first passes through a mode cleaner, which is stabilized to the laser in the same manner as the 40-meter cavities, and is then sent through a single-mode fiber. The mode cleaner is made from mirrors attached to a thermally stable 34-cm long block of ULE glass, and has a bandwidth of 200 kHz. It filters out high-frequency temporal fluctuations in the laser amplitude and wavelength. The beam next passes through the fiber, which couples the laser light into the vacuum system.

(c) Vacuum System

The vacuum system is composed of four 45-cm chambers joined by 20-cm diameter pipes. There are two chambers at the corner of the L. One holds the optical fiber coupler, phase modulator, isolator, and matching lenses; the other holds the suspended beamsplitter mass (which supports the main beamsplitter and steering optics and circulators) and the masses attached to the input cavity mirrors. The end chambers are simpler, holding one suspended test mass each.

Four gate valves at the ends of the pipes allow the tanks to be individually vented to atmosphere without breaking vacuum in the pipes. A system of bellows compensates for the atmospheric force. Each chamber can be run through a cycle of venting, opening for inspection or minor modification, resealing, and pumping, in a few hours. Vacuum is maintained by two 10,000 liter/sec pumps midway down the pipes—one a cryopump, and the other a turbomolecular pump with magnetically levitated bearings. Pressure at the end stations is $4 \cdot 10^{-5}$ torr.

(d) Seismic Isolation, Wire Suspension, and Damping

The prototype is housed in a custom-manufactured building, with separate isolated foundations under each chamber. Optical tables mounted on commercial air springs support the chambers. The bulk of the seismic isolation is achieved by three-layer stacks of lead and rubber inside the chambers, and by the 30-cm long, 80 micron diameter steel wires suspending the test masses. The wires form a pair of slings to support the masses, leaving them free for motions along the cavity axis and constrained against rotation and tilt (Figure H-2).

If left undamped the masses are excited by seismic noise to a pendulation amplitude of 10^{-5} meters peak to peak at the suspension resonance of 1 Hz. The motion would correspond to 10^5 fringe widths or about 10^{11} times the kHz bandwidth displacement sensitivity of the interferometer. These motions are measured with sensors using a light emitting diode, a photodetector and a shadow mask which is placed on the moving mass. The signals from these sensors are combined with the interferometer output and fed back to piezoelectric transducers attached near the suspension points to damp the pendulum motion and to provide the low-frequency gain necessary to maintain optical resonance.

(e) Orientation Control

Figure H-2 also shows how the mass orientation is sensed and controlled [H-2]. Auxiliary Helium-Neon lasers form 40-meter long optical levers with the cavity mirrors

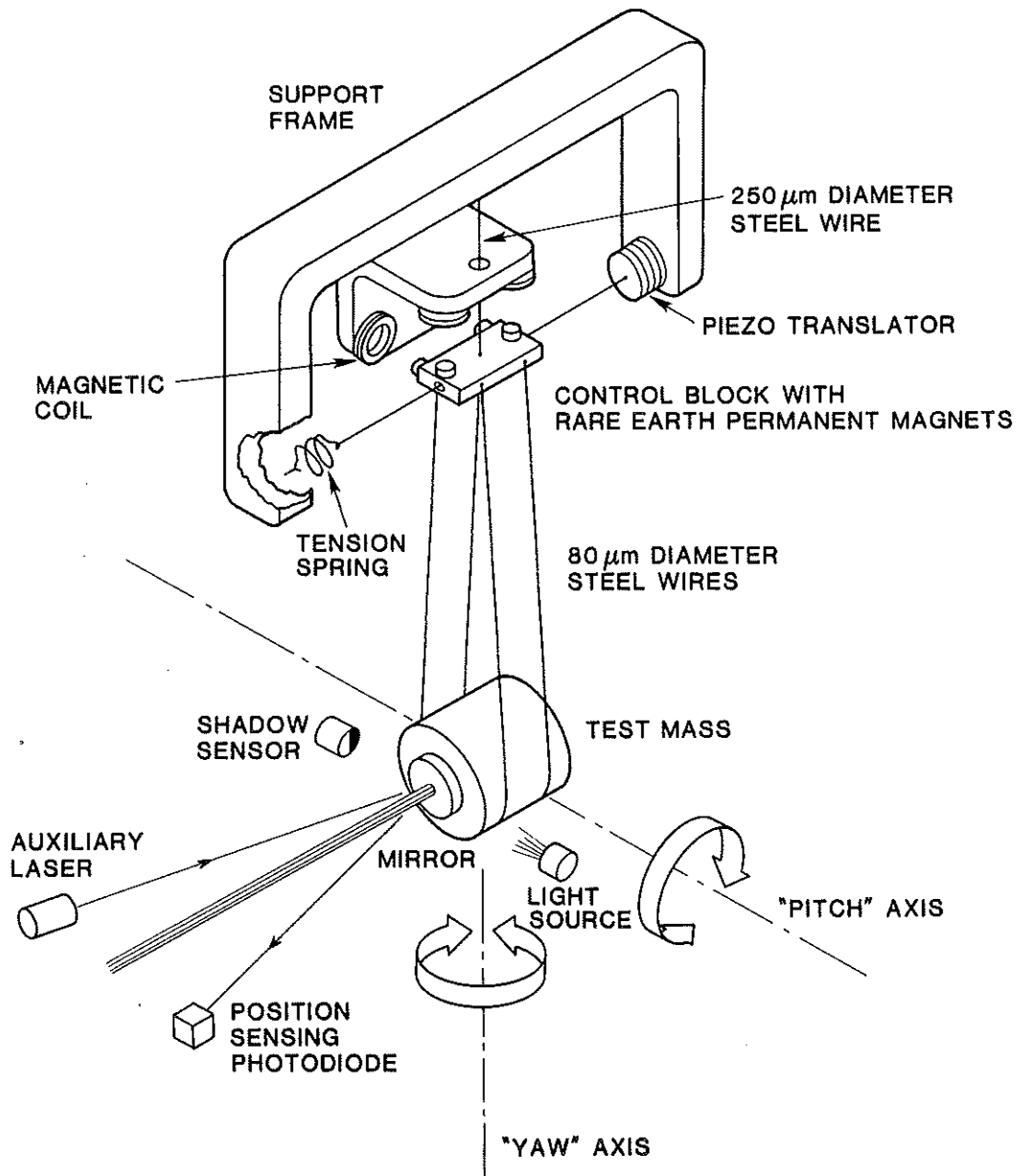


Figure H-2: A schematic drawing of a typical test mass in the 40-meter system, showing the optical lever used for sensing rotation ("yaw") and tilt ("roll") of the mass, and the coils used to apply feedback near the suspension point. The beam from an auxiliary laser at the far end of the pipe strikes the cavity mirror and returns to a two-axis position sensing photodiode. The electrical signal is sent back to coils that interact with magnets on a control block near the suspension point, twisting and turning the block to keep the mass aligned. (The separation between the coils and magnets is exaggerated for clarity; in practice the spacing is adjusted to keep the applied torques insensitive to ground motion.) Also shown are the sensor and translator that damp longitudinal pendulum motions. A modulated beam of light from a light emitting diode is partially blocked by the edge of the mass, producing a spot of light on the photodetector proportional in intensity to the mass's displacement. This signal is filtered, amplified, and applied to a piezoelectric translator at the top, providing cold damping of the pendulum.

to monitor the orientation. The resulting angle signals are fed back to electromagnetic coils near the suspension points to keep the cavities aligned.

(f) Mirrors and Test Masses

The cavity mirrors are made from superpolished fused silica, 3.8 cm diameter by 1 cm thick (see Figure H-3). Multilayer dielectric coatings applied to the surfaces have measured losses due to absorption and scattering of 100 ppm or less. These mirrors store the light long enough to optimize the 40-meter facility for detection of signals as low as 500 Hz.

The mirrors are optically contacted to fused silica masses, 10 cm diameter by 9 cm long. The lowest frequency mode of the mass is 29 kHz, with a Q of $9 \cdot 10^4$. Axial holes of 2.5 cm diameter provide a lossless optical path to the input mirrors.

H.2 Detailed Description of the 1.5-meter Prototype

(a) Structure and Vacuum System

Figure V-6 (Part V) is a photograph of the 1.5 meter prototype gravitational wave detector. It is constructed on two granite tables. The table in the foreground contains the laser and some associated optics; the table in the background supports the vacuum system of the main interferometer. Light is transported between the two tables by means of a single mode optical fiber which serves as a spatial mode filter. The three vertical tanks contain the support points for each of the mirror suspension systems, and the vacuum is maintained at 5×10^{-7} mm Hg by three ion pumps which are cantilevered out from the vertical tanks midway up each tank.

(b) Optics

Figure V-7, Part 5 shows a block diagram of the detector. Each arm of the interferometer is a 56 pass 1.46 meter reentrant optical delay line. The delay line consists of two spherical mirrors facing each other to form a cavity. The beam enters the cavity through a hole in the near mirror and bounces back and forth making a circular pattern of spots on each mirror. When the spot on the near mirror has advanced a multiple of 2π around the circle, it exits from the same hole through which it entered. If the beam is properly mode matched, it is continuously focused by the cavity and the spot size on the mirrors remains constant.

The interferometer is illuminated with light from an argon ion laser operating in a single longitudinal mode at 514.5 nm. The beam passes through a LiTaO₃ crystal where it is phase modulated with wide band noise. The wide band variations of the phase reduce the spatial coherence length of the light so that light scattered out of the main interferometer and onto the photodetector will not cause spurious interference fringes with the main beam. The main beam is unaffected by the modulation because the interferometer is operated near zero path length difference in the two arms (the "white light" fringe).

The beam then passes into a single mode optical fiber. Fluctuations in the angle or position of the beam from the laser are converted by the fiber into intensity fluctuations, to which the interferometer is relatively insensitive. At the output of the fiber the light is mode matched into the delay lines with a commercial zoom lens and passes through a

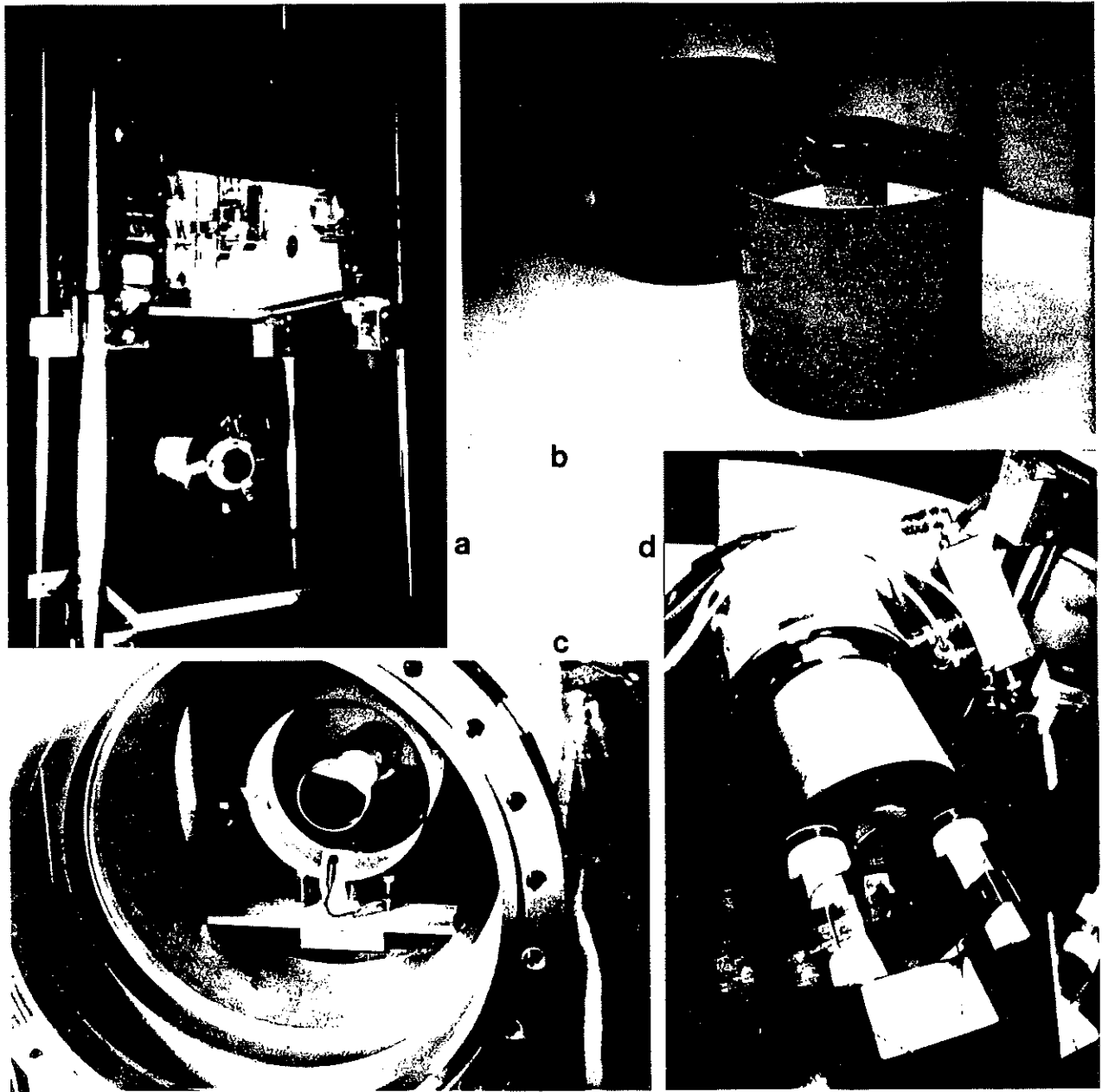


Figure H-3: Views of test masses and suspensions. (a) shows a previous-generation aluminum test mass (ca. 1986). The mirror is glued to a piezoelectric displacement transducer, which in turn is joined by glue to the mass. Also visible are the magnet coils used for orientation controls (cf. Figure H-2) and a lead and rubber stack, seen edge on, supporting the top plate. (b) shows a cavity mirror optically contacted to a fused silica mass. An earlier design made of brass is in the background. (c) shows one of the central masses suspended within its vacuum pipe. The shadowmeter below the mass senses its front edge for damping the 1 Hz pendulum motion. (d) shows an end mass with two types of force transducer: a pair of coils in the front to interact with magnets glued to the mass, and an electrostatic plate that interacts with the back surface, coated to be electrically conducting.

linear polarizer before entering the interferometer. The light must be linearly polarized so that the phase modulation, needed for the fringe interrogation, can be impressed by the AD*P electro-optic crystals at the output of the delay lines. A half-wave retardation plate is used to rotate the plane of polarization of the beam at the input to the fiber to optimize transmission of the fiber in the desired polarization state. The fiber is not polarization preserving, but it has been observed that the fiber will transmit a linearly polarized beam with only a 10% loss to the orthogonal polarization for several days without requiring readjustment. A photodetector after the polarizer provides a signal that can be used to stabilize the amplitude fluctuations of the beam after the fiber, but the additional servo has never been needed.

The output of the interferometer is monitored directly by a photodetector mounted so that the light is incident at Brewster's angle. An experiment is in progress to couple the light out of the interferometer with the same type of optical fiber by which it is injected. The spatial mode apodization performed by the fiber will reduce the contribution from scattering, and improve the contrast.

(c) Suspension

Each end mirror in the 1.5 meter prototype is mounted on a 8 kg aluminum mass suspended by a single wire to form a pendulum with a 2 second period. The 15 kg central mass supports two mirrors, a beam splitter, and two phase modulating crystals. Above the resonance frequency for a particular degree of freedom the mirrors are free to move. Near the resonance frequency the motion of the mirror is sensed and damped in all six degrees of freedom by an electrostatic damping system described below.

(d) Electronics

There are three separate systems in the electronics: an electrostatic mass damping system which controls the motion of the mirrors, a system which performs the fringe interrogation and locking, and another system to collect, store, and interpret the data.

Each aluminum mass supporting a mirror is surrounded on three sides by a cage formed of copper plates evaporated on glass. The position of the mass is sensed relative to the cage by monitoring the capacitances between the mass and the plates. The position information is differentiated to obtain the velocity and a damping signal proportional to velocity is fed back to electrostatically control all six degrees of freedom of each mass.

The interferometer is operated as a gravitational wave detector by holding the path length difference of the two arms constant and near zero. This is accomplished by keeping the system locked to a minimum in the interference fringe at the photodetector. The relative phase of the electric field in each arm is dithered by impressing a high frequency phase modulation on the light with an electrooptic crystal as it exits from each of the delay lines. The output is demodulated and fed back to the phase modulating crystals to maintain the dark fringe. A portion of the demodulated output is also used to move one of the end masses directly at low frequencies to keep the total path length difference within the $\lambda/2$ dynamic range of the phase modulating crystals.

The signal output of the antenna is taken from the error signal used to keep the interferometer on a dark fringe. The error signal is high pass filtered to remove large

low frequency components and then fed into the data collection system, shown in Figure H-4. The data collection system consists of a modified DEC MINC computer system using fast analog to digital converters and a buffered memory. The data stream is then interspersed with information about the state of the system collected at a much slower rate and written to tape. Relative timing for the system is provided by a rubidium clock; absolute timing is achieved by synchronization with WWV. The data collection system is capable of recording approximately 15 minutes of data continuously at 20 kHz and up to 60 minutes at 6 kHz. The data are analyzed offline.

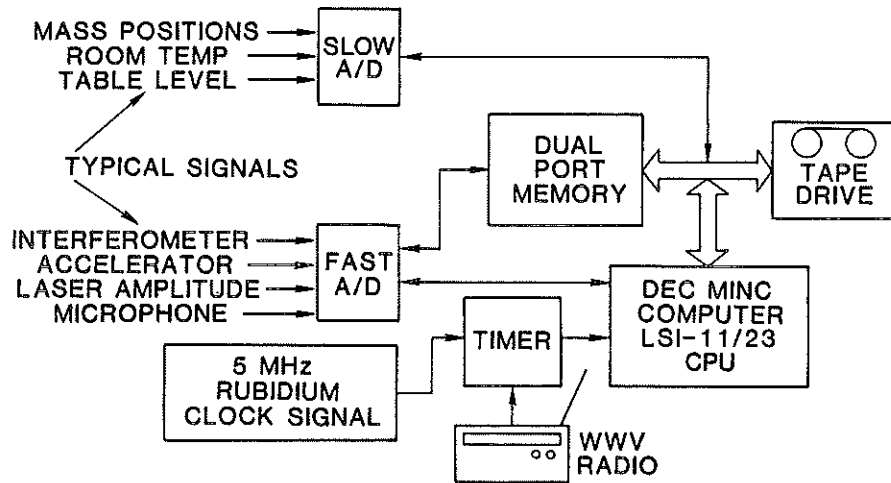


Figure H-4: Block diagram of the data acquisition system for the 1.5 meter prototype.

References

- H-1 A. Rüdiger, R. Schilling, L. Schnupp, W. Winkler, H. Billing, and K. Maischberger, *Optica Acta* **28** (1981), 641-658.
- H-2 S. E. Whitcomb, D. Z. Anderson, R. W. P. Drever, Y. Gursel, M. Hereld, R. Spero *Proceedings of the Third Marcel Grossmann Meeting on General Relativity* ed. Hu Ning, Science Press and North-Holland Publishing Company (1983), 1399.

APPENDIX I
DATA ANALYSIS DEVELOPMENT
AND SEARCHES FOR GRAVITATIONAL RADIATION

1. Introduction

One aspect of the plans for a LIGO which must receive increasing attention is the need to develop techniques to analyze the data. Data reduction techniques are essential to extracting science from the observations, and since the hardware and software requirements are quite substantial it is imperative to begin planning for the necessary resources at an early stage in the design of the LIGO. It is already apparent from the work that has been done that recent technological improvements in data storage should be incorporated, and that even near- future supercomputers must be supplemented by special purpose hardware dedicated to the performance of specific analysis tasks.

We summarize below some of the work that has been done to develop data analysis techniques for interferometers. All of these techniques are directed toward the initial *detection* of a signal of astrophysical origin. Very little work has been done on the problem of optimally extracting the waveforms of the signal (the so called Inverse Problem).

2. Periodic Source: Known Period, Known Position

The 40-meter interferometer was used by Mark Hereld to conduct a search for the millisecond pulsar [I-1] PSR 1937+214 for his Ph.D. thesis [I-2]. The scheme developed by Hereld was to average the output of the detector synchronously with the phase of the pulsar, which could be calculated using the known position. The data were averaged in 30 minute pieces and recorded on tape. Subsequent Fourier analysis yielded narrowband ($0.6 \text{ mHz} = (30 \text{ min})^{-1}$) spectra, centered on the pulsar frequency at 642 Hz and its first harmonic at 1284 Hz. Polarization information was extracted by exploiting the different spatial sensitivity of the antenna to each polarization.

The magnitude of each spectral component was binned and compared with the probability distribution of amplitudes calculated for the noise in the instrument. Figures I-1 and I-2 show the results for the cross polarization at each frequency. The dotted curves show the instrument noise distribution; the vertical lines are the actual data. The arrow identifies the bin that would contain the center of the pulsar spectrum. The conclusion is that the observed spectrum is consistent with noise, with a formal 99.7% confidence sensitivity limit of approximately 1.5×10^{-17} in root mean square (RMS) strain.

3. Pulse Search using Templates

The 1.5-meter prototype was used to look for impulsive events with a set of templates developed by Daniel Dewey for his Ph.D. thesis [I-3]. The idea was to cross-correlate the actual data with an idealized representation of the expected signal and look for statistically significant matches.

Figure I-3 shows the set of 22 templates actually used. The set covers the range of center frequencies for a pulse wave packet from 800 Hz to 5.5 kHz, with a Nyquist

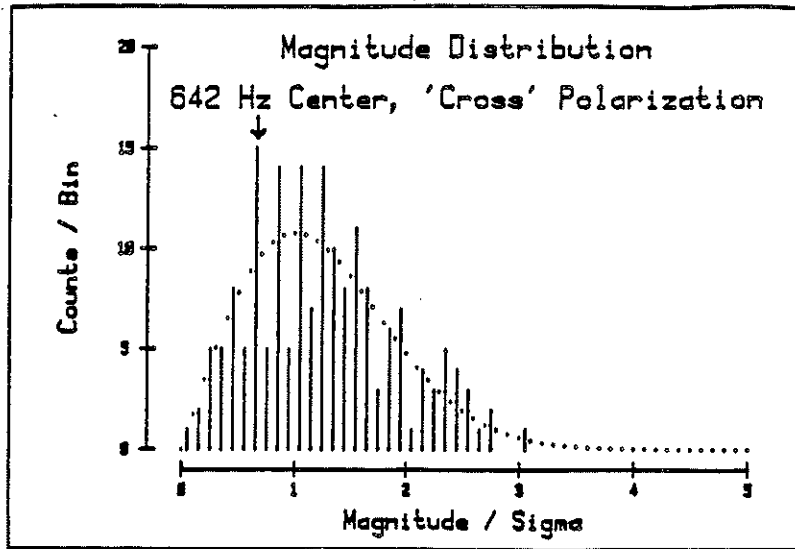


Figure I-1 The measured distribution of the magnitudes of spectral components in a 0.6 mHz wide spectrum centered at the 642 Hz millisecond pulsar frequency. The data were taken with the 40-meter facility and have been processed to extract the "cross" polarization. The dotted line is the noise distribution. The arrow indicates the bin containing the magnitude at the center frequency. (From [I-2], p. 58.)

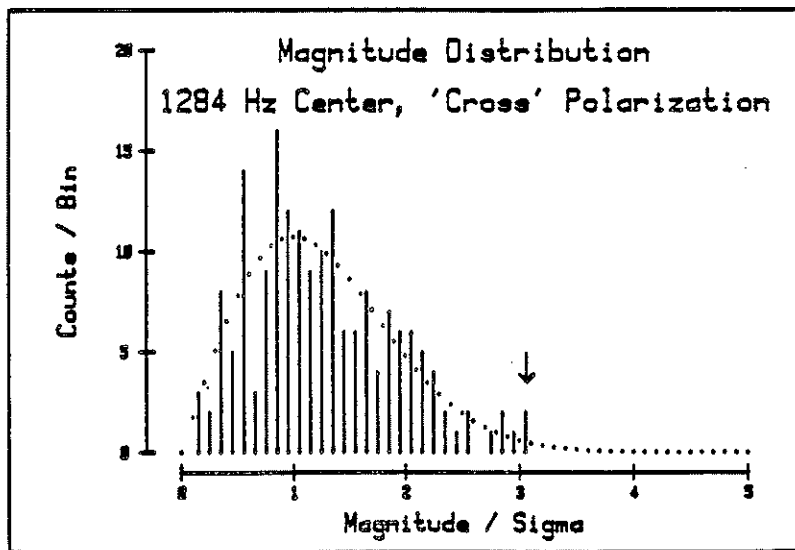


Figure I-2 The measured distribution of the magnitudes of spectral components in a 0.6 mHz wide spectrum centered at the 1284 Hz first harmonic of the millisecond pulsar frequency. The data were taken with the 40-meter facility and have been processed to extract the fixed polarization (the sensitivity to the two polarizations changes as the earth rotates). The dotted line is the noise distribution. The arrow indicates the bin containing the magnitude at the center frequency. (From [I-2], p. 58.)

frequency of 10 kHz. The maximum loss of signal to noise ratio (SNR) due to a mismatch between a real waveform and the idealized representation over this band is 75%. Each cross correlation of a finite length template with the data yields a pulse. The distribution of the amplitudes of these pulses should be a gaussian with variance determined by the

apparatus noise if the receiver noise is gaussian and there are no gravitational wave signals in the data.

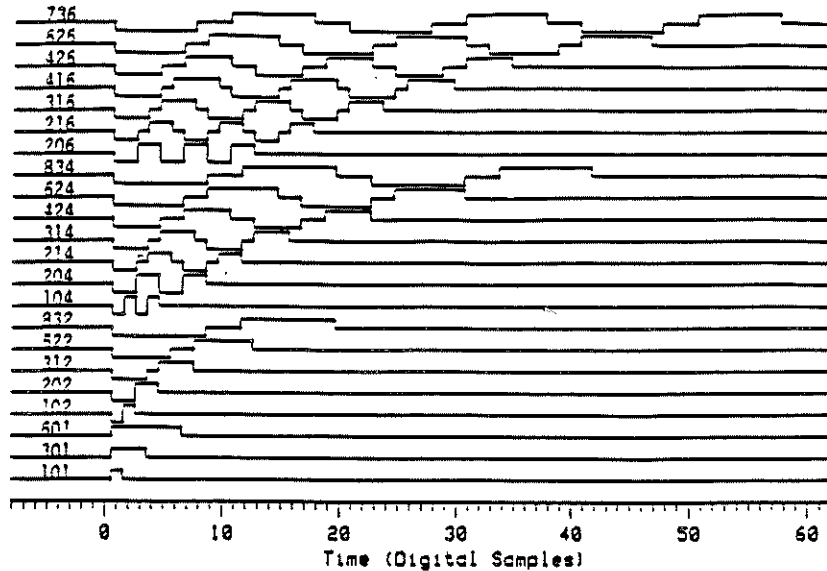


Figure I-3 The set of pulse templates used to search for impulsive events in data from the 1.5-meter facility. The numbers at the left of each template indicate the number of digital samples per cycle for which the template has the value ± 1 , the number of digital samples per cycle for which the template is zero, and the total number of half-cycles for the template. (From [I-3], p. 63.)

Figure I-4 shows the tail of a cumulative pulse height distribution. The slanted dotted line shows the instrument noise distribution, and there is a strong non-gaussian tail beginning at a SNR of approximately 6. Many of these tail events could be associated with electrical transients from the tape drive motor. With these known events removed, the final result was 12 detected events with an RMS strain amplitude $> 5 \times 10^{-14}$, and with an event rate of several per hour. Such events are much too large and too frequent to be of astrophysical origin without being detected in other gravity wave experiments. Such events in a LIGO detector will be removed by cross correlation of the two receivers at the two widely separated sites leaving only gaussian noise.

A similar search for burst sources in data from the recent supernova coincidence experiment is in progress at Caltech as part of Michael Zucker's Ph.D. thesis.

4. Periodic Sources: Unknown Period, Unknown Position

The 1.5-meter interferometer has also been used to conduct a search for periodic sources of unknown period and unknown position, thus exploiting both the broadband character of the detector and its nearly non-directional spatial response. The technique, developed by Jeffrey Livas for his Ph.D. thesis [I-4], is based on Fourier transform methods.

A sinusoidal signal from an astrophysical source is Doppler shifted by the relative motion of the source and antenna, and amplitude modulated by the non-isotropic spatial sensitivity pattern. For a specific position on the sky, the Doppler shift can be removed for all frequencies simultaneously. In principle, the entire sky can be searched

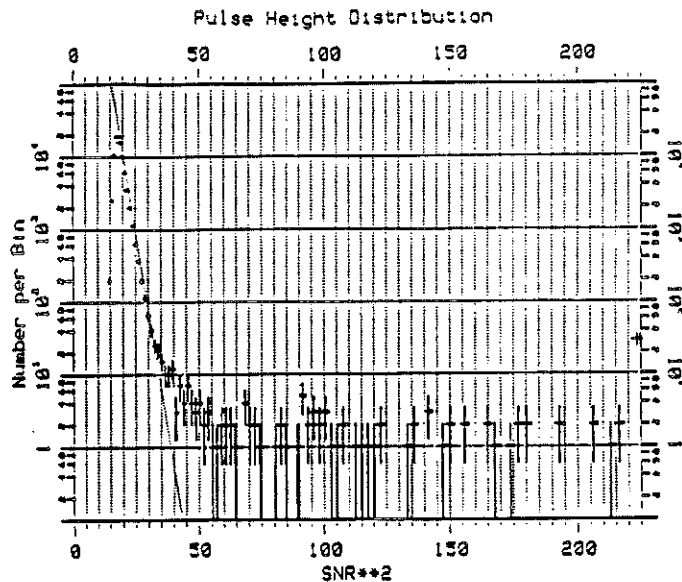


Figure I-4 Tail of the distribution of pulse heights from data filtered with the set of templates in Reference [I-3]. The dotted line shows the noise distribution. Error bars are for statistical counting errors. Events detected in more than one template have been removed, keeping only the pulse height with highest SNR. Most of the events in this tail can be attributed to electrical problems in the magnetic tape drive used to record the data. (From Ref. [I-3], p. 89.)

by repeating the procedure for different positions, but in practice the computational requirements far exceed the capabilities of even future general purpose supercomputers, and will likely require the development of a special-purpose computer.

A complete sky search was accomplished with a series of short (15 minutes of data = 2^{24} points) Fourier transforms taken over a one week baseline, but with limited sensitivity because of the short length of the transforms. However, a Cray 2 supercomputer was required for the computations even at this level. Figure I-5 shows a small portion of one of these transforms, which has a frequency resolution bandwidth of 1 mHz. The obvious peaks in the spectrum were flagged by the detection algorithm, but diagnostics show them to represent resonances in the apparatus, not real signals. Figure I-6 shows the distribution of amplitudes of a complete transform. The solid line is the distribution based on the instrument noise. The arrow indicates the detection threshold.

The final result was an upper limit of approximately $2 \times 10^{-17} (2 \text{ kHz}/f)^2$ in RMS strain in the band from 2-5 kHz, with no signals detected.

5. Template Search for Coalescing Binaries

One of the most promising sources of gravitational radiation is the signal expected from a coalescing binary star system in the final stages of collapse. The expected signal is a chirp whose center frequency increases with time over the duration of the impulse. The waveforms belong to a family of curves that, for fixed polarization (i.e., a detector sensitive only to *one* linear combination of h_+ and h_\times), are a function only of the masses of the constituents. Sheryl Smith at Caltech has developed an algorithm [I-5] to search for this one-parameter family of signals. The data are distorted according to the expected variation of the phase of the waveform, resulting in a sinusoidal waveform if a

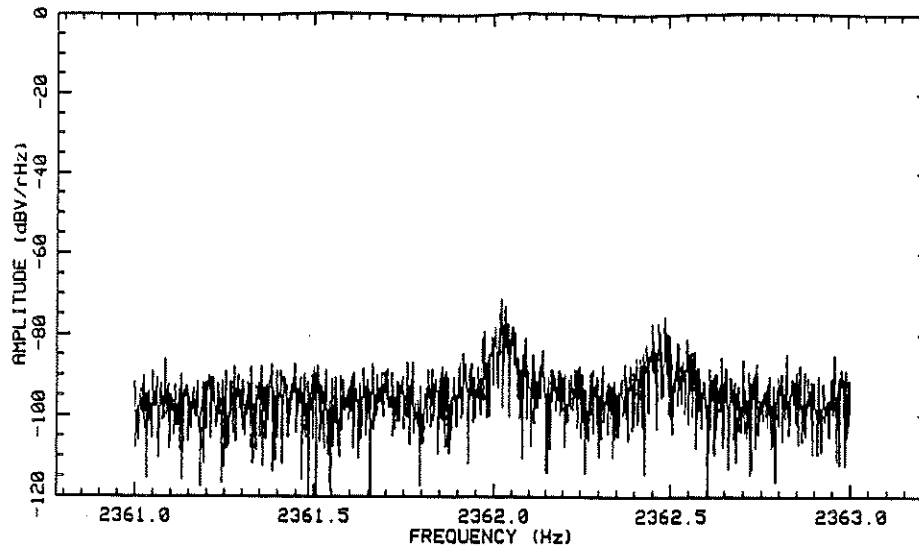


Figure I-5 Small section of a high resolution (1.2 mHz) power spectrum near resonances in the 1.5-meter prototype. Detected on an initial pass through the spectrum, these peaks were identified as apparatus resonances by subsequent diagnostics. (From Ref. [I-4], p. 90.)

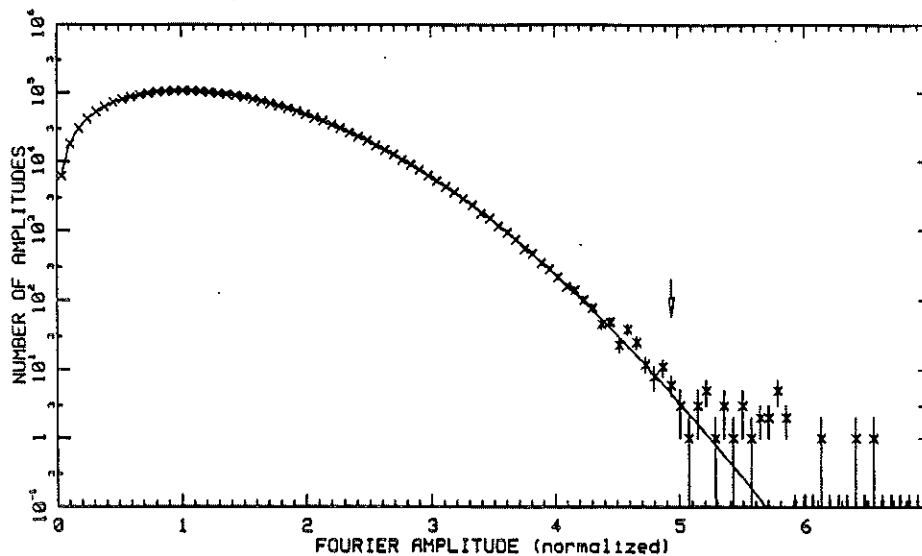


Figure I-6 Measured distribution of the magnitudes of the spectral components of a high resolution power spectrum from 2–5 kHz. Data are from the 1.5-meter facility. The solid line is the expected distribution. The arrow indicates the detection threshold. (From Ref. I-4, p. 84.)

signal is present. The distorted data are then Fourier transformed and the spectrum is searched for statistically significant peaks.

References

- [I-1] Backer, D.C. et. al., *Nature*, **300**, 615, (1982).
- [I-2] Hereld, M. Caltech Ph.D. thesis (1983) Physics, "A Search for Gravitational Radiation from PSR 1937+214"

APPENDIX J

OTHER LIGO EXPERIMENTS AND TECHNOLOGY APPLICATIONS

The major payoffs of the LIGO project will be tests of the laws of gravity and the opening of the new field of gravitational wave astronomy. However, the LIGO facilities may also be useful in other areas of research. The long baseline vacuum system, if augmented in a later phase of the LIGO by closing a triangle within the initial L configuration, will find application in experiments using precision laser gyros. The potential sensitivity and precision of laser gyros built in the LIGO facilities is such that measurement of the predicted "dragging" of the local inertial frame by the earth's rotation may be possible if adequate methods of defining a reference frame are found, and these experiments may set improved limits on more speculative preferred frame effects that occur in many metric theories of gravitation, but not in general relativity. Other methods have been proposed for doing such experiments—mostly in space—and the case for using the LIGO for this is not as strong as the prime objective of gravitational wave research, but the LIGO facilities can provide a unique opportunity for some secondary experiments such as these. Another area of science which could benefit from the LIGO facilities is geophysical research. Direct measurement of ground strain over the LIGO arms may be a useful byproduct of the installations with minor additions to the instrumentation, and the baselines would be longer than those of existing geophysical interferometers. The operation of a high precision laser gyro in the enhanced facilities may give unique possibilities such as measurement of the rotation rate of the tectonic plates on which the facilities are sited or of improved monitoring of fluctuations in the earth's rotation itself.

The high precision metrology demanded by interferometric gravitational wave research has already led to innovative techniques which are being adopted elsewhere. For example a laser frequency stabilization technique devised by us has proved to be one of the most precise methods of controlling laser frequency; it is now being used in areas of precision spectroscopy and is being developed as a frequency standard for space experiments on gravity wave detection. This frequency stabilization technique is spinoff which has already occurred, but many more of the precise laser beam control, pointing, and aligning techniques being developed in the LIGO project are also likely to have wide application. The development of moderate power, 10 to 100 watt, laser systems with exquisite spectral purity, less than 10^{-4} Hz / $\sqrt{\text{Hz}}$, and amplitude fluctuations at the Poisson limit will find application in communications and precision instrumentation.

Gravitational wave research requires broadband vibration isolation systems operating near the thermal noise limit; the development of these systems has broad application in other areas requiring stability at submicron levels, such as semiconductor chip masking and processing and electron and tunneling microscopy. Members of the LIGO project have been frequently asked to assist in vibration isolation problems. Associated with the vibration isolation technology is our development of economical and precise position sensors using optical fiber and integrated optics technology. These sensors will have application in general instrumentation, precision machine tools and robotics.

There are several areas in which the LIGO project will give impetus to technological innovation and development because of its special needs. The stringent requirements for mirror grinding, polishing and coatings can now be met in industry for the initial LIGO receiver designs but the continuing improvement of receivers will push the development of optics with lower scattering and lower loss.

The data analysis for periodic sources of unknown location and oscillation period is a substantial problem even for supercomputers. The solution of the problem will require both hardware and software innovation.